UNIVERSITÀ DEGLI STUDI DI SASSARI

SCUOLA DI DOTTORATO DI RICERCA
Scienze e Biotecnologie
dei Sistemi Agrari e Forestali
e delle Produzioni Alimentari

Biotecnologie microbiche agroalimentari

Ciclo XXV

Modulating the release properties of active compounds from packaging materials by a physicochemical/nanotechnology approach

Dr. Carlo Alessio Cozzolino

Direttore della Scuola	Prof.ssa Alba Pusino
Referente di Indirizzo	Prof.ssa Marilena Budroni
Docente Guida	Prof. Antonio Piga
Tutor	Prof. Luciano Piergiovanni
Co-tutor	Dr. Stefano Farris

Anno accademico 2011- 2012

MODULATING THE RELEASE PROPERTIES OF ACTIVE COMPOUNDS FROM PACKAGING MATERIALS BY A PHYSICOCHEMICAL/NANOTECHNOLOGY APPROACH

Dipartimento di Agraria
University of Sassari

In collaboration with Packlab – Defens, University of Milan

CARLO ALESSIO COZZOLINO

Doctoral Thesis

Sassari 2012

Turn On, Tune In, Drop Out

[Timothy Leary]

MODULATING THE RELEASE PROPERTIES OF ACTIVE COMPOUNDS FROM PACKAGING MATERIALS BY A PHYSICOCHEMICAL/NANOTECHNOLOGY APPROACH

Carlo Alessio Cozzolino

STAA, Department of Agriculture - University of Sassari

ABSTRACT

Controlled release system (CRS) is a new generation of release systems that can release active molecules at different controlled rates for enhancing the quality and safety of foods during storage. One critical point is to maintain a concentration of the active molecule to a predetermined level over a required time span. The different controlled rates are influenced by the distribution of the active molecule across the polymer matrix and 'active molecule-polymer matrix interactions', besides the effect of external triggers (pH, temperature, humidity). This is why a deep knowledge of the active compound release is necessary.

The research activity carried out during these three years focused on three main topics, namely:

I. investigation of the release kinetics of a model drug-like compound (Coomassie brilliant blue) from polyvinyl alcohol (PVOH) films into a hydro-alcoholic solution as a function of the physicochemical properties of the polymer matrix;
II. study of a cellulose-based matrix (MFC) for the release of lysozyme.

The results obtained can be profitably used for the development of delivery systems for different applications (e.g. food packaging), where the controlled release over time of an active molecule is the target. Moreover, these studies have shown the possibility of using a green and nanotechnology approach (through the use of MFC) for the development of CRS.

Finally, branches from the aforementioned two topics led to further research, grouped in three main sub-topics:

III. development of a 'wetting enhancer' pullulan coating for antifog packaging applications;
IV. development of pullulan films reinforced with MFC;
V. study of a gelatin-based matrix for the release of a soluble compound (Lauric arginate ethyl ester LAE).

Overall, these topics prompted an advancement in the field of bio-based materials, as they investigated new approaches for a suitable and feasible exploitation of biopolymers for applications that are beyond the development of controlled release systems.

LIST OF PAPERS

This PhD thesis is based on the following papers:

I. Dye release behavior from polyvinyl alcohol films in a hydro-alcoholic medium: influence of physicochemical heterogeneity.
Cozzolino C.A., Blomfeldt T. O.J., Nilsson F., Piga A., Piergiovanni L., Farris S.
Colloids and Surfaces A: Physicochemical and Engineering Aspects, 2012, 403: 45– 53

II. Exploiting the nano-sized features of microfibrillated cellulose (MFC) for the development of controlled release packaging.
Cozzolino C.A., Nilsson F., Iotti M., Piga A., Farris S.
Submitted to the Colloids and Surfaces B: Biointerfaces, 2012

Other works done in these three years are:

III. 'Wetting enhancer' pullulan coating for anti-fog packaging applications.
Introzzi L., Fuentes-Alventosa J.M., Cozzolino C.A., Trabattoni S., Tavazzi S., Schiraldi A., Piergiovanni L., Farris S.
Applied Materials & Interfaces, 2012, 4: 3692−3700.

IV. A green nanocomposite: Pullulan Films Reinforced with MFC.
Cozzolino C.A., Piga A., Farris S.
Manuscript, 2012

V. Qualità e sicurezza dei prodotti vegetali minimamente trattati (IV gamma) attraverso imballaggi plastici funzionali.
Quaderni della Ricerca, 2012, vol. 143. Regione Lombardia Agricoltura. [VEGAPACK PROJECT]

TABLE OF CONTENTS

1 PURPOSE OF THE STUDY

The overall purpose of this research was to investigate the mechanisms underlying the release of an active compound from a polymer matrix, in order to then develop a controlled release system (CRS) packaging material. CRS indicates a new generation of release systems that can release active molecules at different controlled rates for enhancing the quality and safety of foods during storage. One critical point is to maintain a concentration of active molecule, within the matrix, to a predetermined level over a required time span. For this reason is necessary a deep knowledge of the distribution of the active molecule across the polymer matrix and 'active molecule-polymer matrix interactions', besides the effect of external triggers (pH, temperature, humidity), that will influence the different controlled rates (Paper I & II).

In the first part of this research, the goal was to assess the influence of physicochemical parameters on the release properties of a polymer system including the active molecule. To this scope, poly-vinyl alcohol (PVOH) was used as polymer matrix, while an anionic low molecular weight dye was used as the model drug-like active compound. The release in a hydro-alcoholic medium was studied as a function of molecular weight (MW) and degree of hydrolysis (DH) (Paper I). The hydro-alcoholic medium was selected because this is often encountered in the everyday life (e.g. food, drinks, cosmetics, and health care products). Moreover, water/ethanol solutions are food simulants within the food contact material legislation.

The second part of my project concerned the experience carried out in Norway at Paper and Fibre Research Institute (PFI) and at Norwegian University of Science and Technology (NTNU). The goal of this study was to develop a controlled release system based on microfibrillated cellulose (MFC) as the carrying polymer and lysozyme as the antimicrobial agent, specifically intended for food packaging applications (Paper II). The rationale is that using MFC might help retain the active molecule within the polymer matrix, thus preventing its almost complete loss (i.e., 100% release) in a few times. The reason for such reduced release lies in the 'interface effect' arising from the nano-dimensional structure of the polymer network, which would allow establishing a larger number of polymer-active molecule

interactions (i.e., electrostatic forces) compared to macro-sized networks such as paper/paperboard or plastics (see Figure 1). Towards this scope, the release kinetics of lysozyme from MFC films were investigated by estimating a quantifiable parameter (i.e. the diffusion coefficient) as a function of two food simulants (simulant A – water, and simulant C – water/ethanol 10 wt.%) at two different temperatures (6°C and 23°C). The release kinetics of the active compound were also estimated in presence of two release-modulating agents, namely glycerol and sodium chloride.

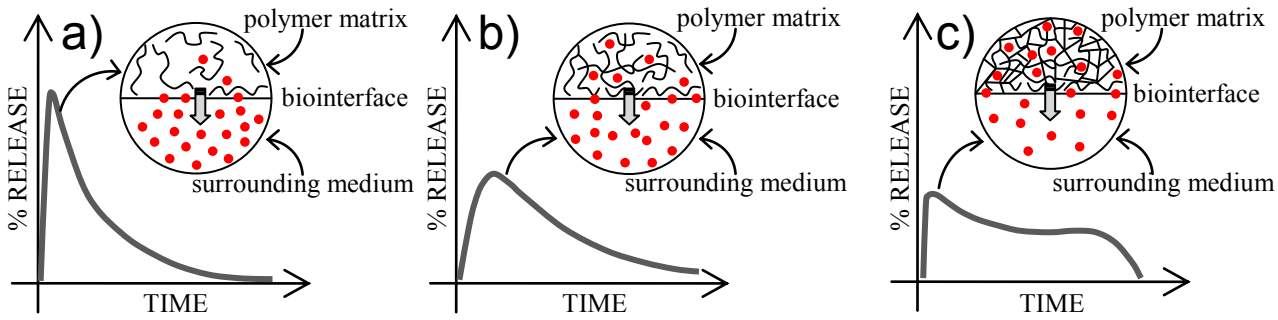

Figure 1. 'Interface effect' arising from the nano-dimensional structure of the polymer network.

The third part of my thesis concerned, briefly, other works done in these three years, such as the development of "wetting enhancer" pullulan coatings for antifog packaging applications (Paper III), the development of pullulan films reinforced with MFC (Paper IV) and Vegapack project, to optimize the quality and safety of minimally processed vegetable products (Paper V).

2 INTRODUCTION

2.1 A point of view

The interest in polymer systems with tunable release properties has dramatically increased over recent years. The reason for this success is that CRS turned to be an appealing topic since it has been developed, as you can see in Figures 2-3. This is also likely because of the growing attention to this intriguing topic by sectors that traditionally lagged behind long established fields, such as the pharmaceutical and biomedical industries. Among others, the packaging field, especially referring to food applications, is experiencing new, exciting progress mainly driven by the expanding consumer demands and industrial production trends towards minimally processed, fresh, tasty, and convenient food products with extended shelf–life and controlled quality. New and alternative food packaging technologies are expected to be developed in the coming years for controlling both microbial contamination and detrimental oxidation of foods, in order to limit, inhibit or delay the growth of microorganisms and the rate of quality decay. Among other approaches, some of which are carbon dioxide absorbers, anti-fogging films, flavour absorbing films and ethanol emitters as shown in Table 1, the development of active packaging systems foresees the incorporation of active substances in either the bulk materials or coatings (Dainelli *et al*., 2008). Such active compounds, similar to drugs loaded into pharmaceutical capsules, will be then released to the target body (i.e. the food) in order to inhibit or control some undesirable reactions (e.g. microbial spoilage, lipid oxidation, enzymatic browning, etc.) that may accelerate the quality decay of the food matrix. Besides the purpose of shelf-life extension, this approach also makes it possible to avoid any direct addition of preservatives into the food matrix (LaCoste *et al*., 2005). However, the active compounds should not be delivered too rapidly, as the desired effect (e.g. antimicrobial, antioxidant, etc.) would be limited to a narrow temporal window, with no significant improvement in terms of shelf-life extension (Zhang *et al*., 2004; Li *et al*., 2006). Any mechanism allowing the release of active compounds in a deliberately controlled manner, i.e. at different rates, can be referred to as controlled release packaging (CRP) or controlled release system (CRS). Although technically sound, obtaining effective controlled release packaging has been demonstrated to be a difficult task, as many factors need to be simultaneously considered, such as the distribution of the active compound across the thickness of the film/coating, the “active compound-polymer interactions”, and the effect

of external triggers. There are three main strategies to control the delivery of active molecules: i) the development of multi-component structures, i.e. polymer matrices obtained by blending two (or more) phases, sometimes needing a third minor component acting as compatibilizer [Tunç and Duman, 2011); ii) the generation of highly smart structures by acting on the morphology of the polymer matrix entrapping the active molecules (Gemili *et al*., 2010); iii) the change of the chemical structure of polymer matrices by the introduction of new functional groups that are able to interact with the active compounds according to a designed pattern, thus controlling their release over time (Onofre *et al*., 2009; Yilmaz *et al*., 2002). However, these approaches involve complex release systems that, while claimed as effective, actually incur high production costs, thus rendering them unfeasible for many applications and impeding market opportunity. Therefore, new strategies are needed to promote the penetration of CRP/CRS into "cheap" markets (such as food packaging) through efficient and cost-effective solutions, and, in the case of food packaging, considering the Regulation 1935/2004/EC and new Regulation 450/2009/EC regarding the general requirements and specific safety and marketing issues related to active and intelligent packaging (Restuccia *et al*., 2010).

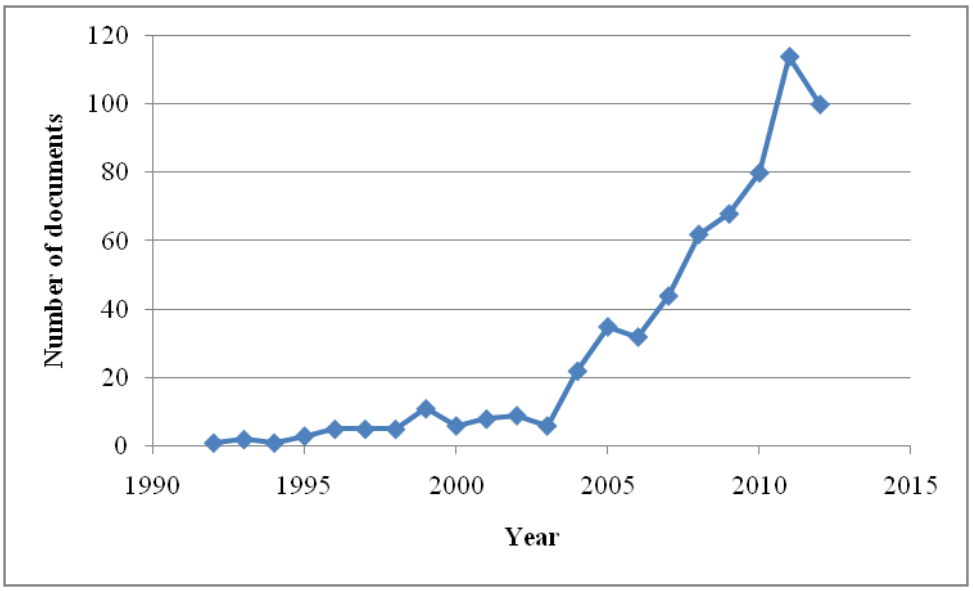

Figure 2. Number of document/year; Query: "tunable release" [Sciverse Scopus, October 2012].

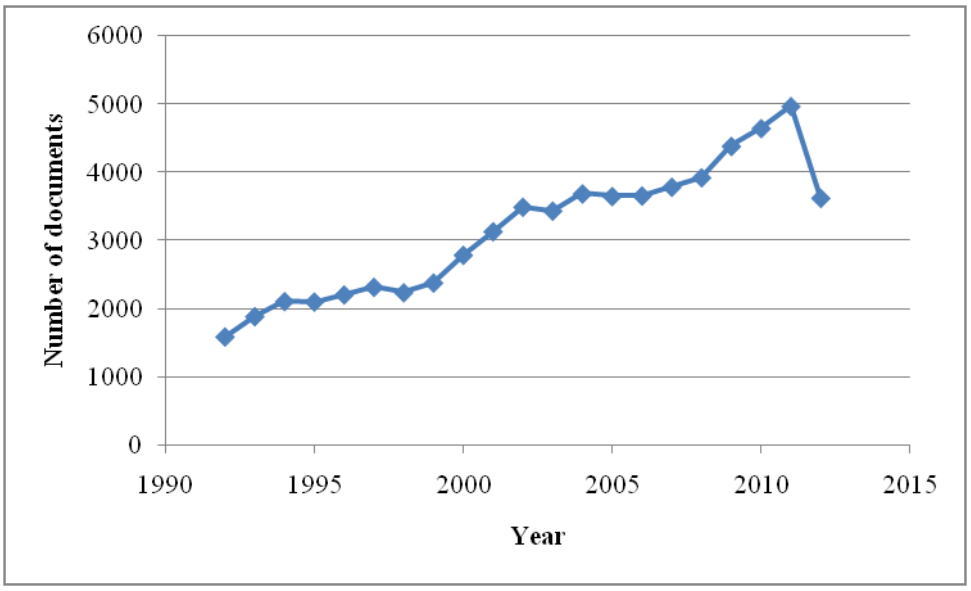

Figure 3. Number of document/year; Query: "controlled release system" [Sciverse Scopus, October 2012].

Type of application	Foods
Antimicrobial releasing films	Dry apricots
Antioxidant releasing films	Cereals
Anti-fogging films	Some fresh fruit and vegetable packages
Anti-sticking films	Soft candies, cheese slices
Carbon dioxide absorbers	Ground coffee
Carbon dioxide emitters	Fish, meat
Color containing films	Surimi
Ethylene scavengers	Banana, avocados, kiwifruit
Ethanol emitters	Cakes, bread, fish
Flavour absorbing films	Navel orange juice
Flavour releasing films	Ground coffee
Gas permeable/breathable films	Ready-to-eat salads
Light absorbers	Milk, pizza
Microwave susceptors	Ready-to-eat meals
Moisture absorbers	Dry and dehydrated products, fish, meat, poultry
Oxygen scavengers	Fish, meat, cheese, bread, cakes, pizza, ground coffee, tea, chocolate, beer, refrigerated pasta, potato chips, powdered drink, roasted nuts, fruit tortes
Time-temperature indicators	Refrigerated pasta, microwaveable pancake syrup

Table 1. Applications of active packaging technologies (adapted from Restuccia *et al.*, 2010).

2.2 Why PVOH?

Polyvinyl alcohol (PVOH) is an attractive polymer for many different applications. It has been widely used in many fields, such as: biomedical, as a scaffold supporting material for tissue engineering applications [Asran *et al*., 2010]; pharmaceutical, for the obtainment of wound-dressing systems [Sung *et al*., 2010] and environmental, for the production of films for the removal of heavy metal ions in water [Wu *et al*., 2010]. Other applications include packaging [Marino *et al*., 2008], agriculture [De Prisco *et al*., 2002], electrochemistry [Boroglu *et al*., 2011] and fuel cells [Yun *et al*., 2011]. In addition, PVOH is well suited both to develop polymer blends in association with many biopolymers [Park *et al*., 2001; Liang *et al*., 2009; Chiellini *et al*., 2008; Sudhamani *et al*., 2003; Dicharry *et al*., 2003] and to produce electrospun nanofibrous mats [Nirmala *et al*., 2011]. The success of PVOH is due to many reasons, first of all because of its unique molecular structure and properties, such as its rubbery or elastic nature and its high degree of swelling in aqueous solutions [Kobayashi *et al*., 2003]. Moreover, the hydroxyl pendant group on every second carbon atom on its backbone allows PVOH to take part in many chemical cross-linking reactions [Moreno *et al*., 2010], interact with many other polymers, primarily through hydrogen bonding [Labuschagne *et al*., 2008], and form a physical hydrogel through the well-known freeze-thaw process [Poursamar *et al*., 2011]. Inherent non-toxicity, non-carcinogenicity, and good biocompatibility represent additional desirable features. Finally, PVOH is the only known purely C-C macromolecule that can be biodegraded [Kaplan *et al*., 1993]. One of the main interests in PVOH-based polymer systems lies in the development of smart devices with tunable release properties. In this respect, long established fields of application are the pharmaceutical and biomedical industries, where PVOH has been extensively used as a privileged polymer for the encapsulation/ loading and the subsequent release of enzymes [Moreno *et al*., 2011], proteins [Li *et al*., 1998], cells [Schwenter *et al*., 2004] and, more broadly, a huge variety of drugs [Huang *et al*., 2000; Shaheen and Yamaura, 2002; Jin and Hsieh, 2005; Juntanon *et al*., 2008]. However, the field of sustained delivery of active compounds is advancing rapidly, and new applications within sectors that traditionally lagged behind the aforementioned established fields came about during the last decades. Among others, novel release systems are expected to grow in the coming years within the food packaging field, due to the increasing interest toward the concept of active packaging [Dainelli *et al*., 2008]. The underlying basic idea is to convey an active molecule (e.g.

anitimicrobial, antioxidant, etc.) from the polymeric reservoir to the target body (i.e. the food), maintaining its concentration to a predetermined level over a required time span. This can be accomplished if the polymer system 'senses' and 'responds' to specific stimuli, such as temperature [Liu *et al*., 2011], pH [Jin *et al*., 2005; Klee *et al*., 2009], surrounding medium [Yeh *et al*., 2011], light [Costa *et al*., 2011], electric field [Juntanon *et al*., 2008; Yun *et al*., 2010] and ultrasound [Small *et al*., 2011], which act as triggers. The main relevant advantage of this approach is that it allows avoidance of either multiple supplies or direct addition of a large amount of the active compound directly into the target body. However, to make release systems work efficiently, controlling the delivery rate over time in a deliberate manner is the crucial point. This is why 'controlled release system' (CRS) appears in most cases a more appropriate definition. In light of these considerations, both the comprehension of the phenomena underlying the release process and the description of the release kinetics through mathematical models appear necessary steps for the design and development of any controlled delivery device.

2.3 Why MFC?

Due to environment and sustainability issues, recent years have seen a increasingly attention in green technology, particularly in the field of materials science through the development of bio- and bionano- composites [Siqueira *et al*., 2010; Faruk *et al*., 2012; Klemm *et al*., 2011]. Cellulose is one of the most important polysaccharides and abundant biopolymers on earth [Siró and Plackett, 2010], which provides mechanical properties to higher plant cell [Alen, 2000]. It consists of a linear β-glucose homopolymer with subunits called cellobiose, β-1,4 linked glucose [Cabiaca *et al*., 2011]. The cellulose chains are arranged in strands of cellulose microfibrils [Berglund, 2006] that are partially crystalline, where the crystalline parts are held together by hydrogen bonding and van der Waals forces, immersed in a matrix of hemicellulose and lignin. Cellulose fibres can also be disintegrated into their structural nano-components [Chinga-Carrasco *et al*., 2011] -cellulose nanoparticles (CNs)- such as microfibrillated cellulose (MFC), nanofibrilated cellulose (NFC) and cellulose nanocrystal (CNC), different from each other as regards size, aspect ratio, morphology, crystallinity, crystal structure and properties [Moon *et al*., 2011]. In the field of nanocomposites, CNs are ideal materials on which to base a new biopolymer composites industry [Moon *et al*., 2011]. Microfibrils are important fiber wall components. All plants and some kinds of bacteria,

tunicates and algae produce cellulose [Klemm *et al*., 2006]. Cellulose-based materials, such as microfibrillated cellulose (MFC), have captured much attention for their renewable, recyclable, compostable and biodegradable properties [Hult *et al*., 2010]. Early studies on the MFC from wood fibers date back to the 80's [Turbak *et al*., 1983]. At that time, MFC was obtained by the disintegration of cellulose fibers by means of high shear forces. This procedure resulted in the production of a highly entangled network consisting of nano-size elements, with a gel-like behavior of diluted (< 1 wt.%) MFC water dispersions [Turbak *et al*., 1983; Iotti *et al*., 2011; Herrick *et al*., 1983]. In literature there are several terms to describe the MFC, including: nanofiber [Abe *et al*., 2007], microfibril aggregates [Iwamoto *et al*., 2007], microfibrils [Aulin *et al*., 2008], , nanofibril [Ahola *et al*., 2008], nanofibrillar cellulose [Pääkkö *et al*., 2008], fibril aggregates [Virtanen *et al*., 2008] and microfibrillar cellulose [Syverud and Stenius, 2009]. According to the conventional nomenclature, which states that the term nano should be referred to as 'having a size between 0.001 and 0.1 microns (1 to 100 nm)', MFC can be regarded as nano-fibrils with diameters of roughly less than 100 nm, lengths of several micrometers [Chinga-Carrasco, 2011; Syveruda, *et al*., 2011] and an aspect ratio (L/d) in the range of 100-150 [Hubbe *et al*., 2008]. MFC are composed of amorphous and crystalline regions [Chinga-Carrasco, 2011] that, together with both large specific surface area and reactive OH-groups [Syveruda *et al*., 2011], contribute to the excellent mechanical properties, such as stiffness and tensile strength [Lu *et al*., 2008], that have been exploited so far for several purposes [Ahola *et al*., 2008]. Applications of MFC include, but are not limited to: reinforcement in nanocomposite materials [López-Rubio *et al*., 2007; , Srithep *et al*., 2012], dispersion stabilizers [Andresen and. Stenius, 2007], filtration media [Burger *et al*., 2006], and oxygen barrier material in food and pharmaceutical application [Syverud and Stenius, 2009]. However, very few works dealing with the development of active materials based on MFC, especially intended for antimicrobial applications, have been reported [Andresen *et al*., 2007; Martins *et al*., 2012].

In this respect, the past decade has witnessed to a rapid increase in works concerning the development of active films intended for food packaging applications, with special emphasis on alternative methods for controlling both microbial contamination and detrimental oxidation of foods in order to limit, inhibit or delay the growth of microorganisms and the rate of quality decay [Joerger , 2007; Quintavalla and Vicini, 2002; Rodríguez *et al*., 2007]. Toward this goal, it has previously been demonstrated that achieving the controlled release of active

molecules over time is the key for the shelf life extension of perishable foods [LaCoste *et al*., 2005]. Controlled release packaging (CRP), i.e. the slow and modulated release of active compounds from package to food, has been proven to be more effective than adding active compounds directly into food formulation [Balasubramanian *et al*., 2011]. However, despite many attempts, achieving an effective CRP system is still a tricky task. Among other strategies (i.e. modification of packaging polymer structure or encapsulation of the active compounds) the physicochemical interactions between polymer matrix and loaded molecule may dictate the ultimate release attributes of the packaging system [Cozzolino *et al*., 2012]. In particular, exploiting electrostatic forces between polymer and active molecule has been suggested as a valid approach to obtain new composites with tailored features (e.g. the release properties) [Martins *et al*., 2012; S. Farris *et al*., 2009]. Bearing this in mind, the use of MFC (which carries an overall negative charge) and the enzyme lysozyme (which carries an overall positive charge for pH below its isoelectric point, i.e. pH<10.7) can be seen as a profitable association to generate new biocomposites with tailored antimicrobial properties. Lysozyme has received great attention during the last years as a natural biopreservative for antimicrobial packaging applications [Mascheroni *et al*., 2010; Ibrahim *et al*., 1996], and it has already been classified as a food additive by the European Directive 95/2/EC. Its antimicrobial activity has to be ascribed to the hydrolysis of the cell wall of Gram-positive and, to a less extent, Gram-negative bacteria [Ibrahim *et al*., 1996]. However, previous studies on lysozyme-based active packaging systems suggested that, despite their antimicrobial efficacy, the antimicrobial effect was limited to a short time mainly due to a too fast delivery from the polymer network [Gemili *et al*., 2009].

3 EXPERIMENTAL

3.1 Materials & Chemicals

3.1.1 Paper I

Three different types of polyvinyl alcohol (Fluka Analytical, Milan, Italy) in the form of pellets were used in this work: 1) PVOH 4-88, with DH 86.7–88.7 mol%; MW ~31,000; viscosity (4% aqueous solution at 20°C) 3.5–4.5 mPa s; degree of polymerization ~630; ester number 130–150; 2) PVOH 40-88, with DH 86.7–88.7 mol%; MW ~205,000; viscosity (4% aqueous solution at 20°C) 38–42 mPa s; degree of polymerization ~4200; ester number 130–150; 3) PVOH 10-98, with DH 98.0–98.8 mol%; MW ~61,000; viscosity (4% aqueous solution at 20°C) 9–11 mPa s; degree of polymerization ~1400; ester number 15–25. Coomassie Brilliant Blue G-250 (Figure 4) (sodium 3-[[4-[(E)-[4-(4-ethoxyanilino)phenyl]-[4-[ethyl-[(3-sulfonatophenyl)methyl]azaniumylidene]-2-methylcyclohexa-2,5-dien-1-ylidene]methyl]- -ethyl-3-methylanilino]methyl]benzenesulfonate; molecular weight=854.02 Da; maximum absorbance λmax=610 nm) – Sigma Aldrich, Milan, Italy), was used as the model active compound. Milli-Q water (18.3 MΩ cm) and ethanol (purity ≥99.8%, Fluka Analytical, Milan, Italy) were used for the preparation of the hydro-alcoholic polymer–dye solutions.

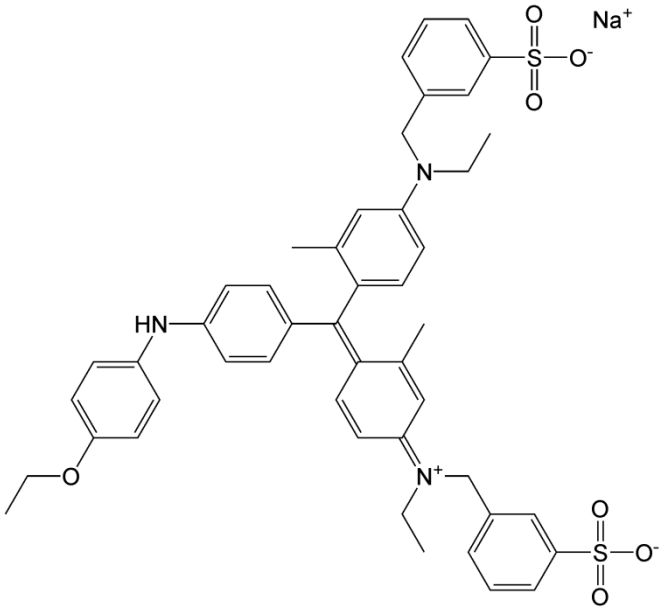

Figure 4. Chemical structure of the Coomassie Brilliant Blue G dye used in this work as the model drug-like compound for the release study.

3.1.2 Paper II

Microfibrillar cellulose was produced at the Paper and Fibre Research Institute (PFI, Trondheim, Norway) by two different types of cellulose: (I) ECF (elemental chlorine free) fully bleached sulphate pulp mainly based on juvenile *Picea abies* and (II) ECF (elemental chlorine free) fully bleached sulphate cellulose mainly based on mature *Picea abies* with up to 5wt.% pine (*Pinus sylvestris*), according to the same manufacturing procedure described by Turbak and Herrik [Turbak *et al*., 1983; Herrick *et al*., 1983]. The main physicochemical characteristics of the obtained MFC were described in previous papers [Iotti *et al*., 2011; Syverud and Stenius, 2009]. Lysozyme (Figure 5) from chicken egg white powder (crystalline; ~70000 units/mg) was purchased from Sigma-Aldrich (Oslo, Norway). Glycerol (redistilled, min 99.5%$^{w}/_{v}$) was purchased from VWR International (Leuven, Belgium). Sodium chloride was purchased from Merck (Darmstadt, Germany). Milli-Q water with a resistivity higher than 18.2 MΩ cm and ethanol (Fluka Analytical, Oslo, Norway) were used for the preparation of the hydro-alcoholic solutions (water/ethanol 10 wt.%).

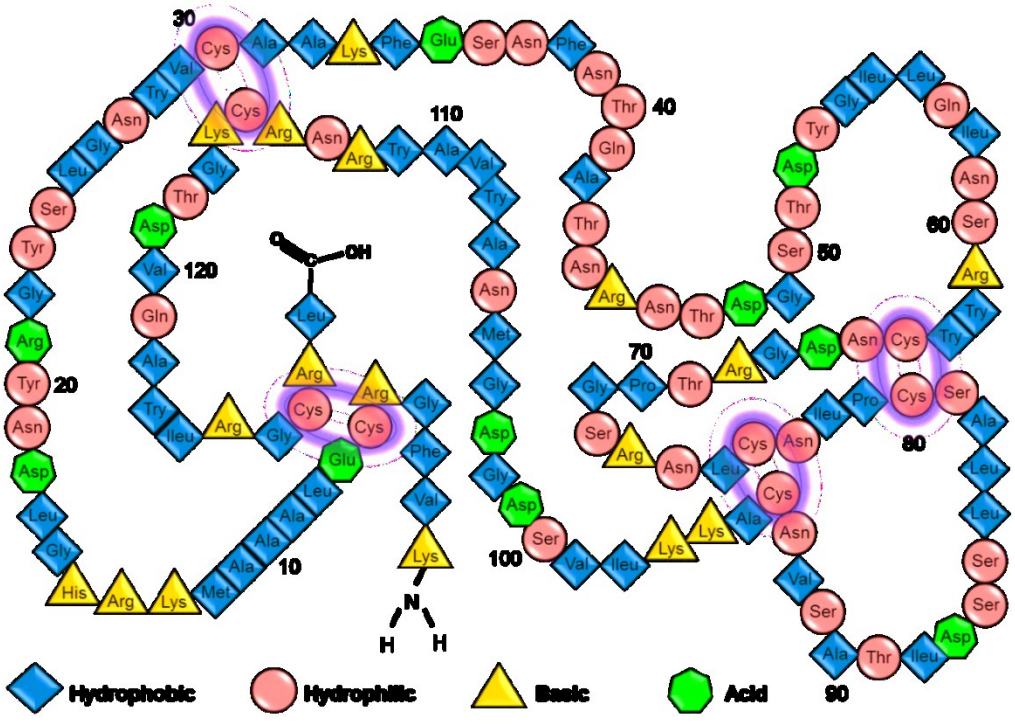

Figure 5. Schematic representation of the structure of egg white lysozyme, with in evidence the four disulfide bonds and the nature (hydrophilic, hydrophobic, basic, acid) of the amino acids sequence (adapted from Canfield and Liu, 1965).

3.2 Sample Preparation

3.2.1 Paper I

The PVOH water solutions were prepared by dissolving 5 g of PVOH in 95 mL of hot water (92°C) for 1 h under gentle stirring (500 rpm). After cooling at room temperature, the film-forming solutions (pH = 5.5 ± 0.1) were loaded with the dye powder (0.052% weight of dye/weight of dry polymer), which dissolved rapidly under gentle stirring. At this pH, the dye molecules carry a net negative charge [Chial *et al*., 1993] (Figure 4). Next, 5 g of the obtained solutions were poured on glass Petri plates (6 cm in diameter) and dried in an oven at 55°C for 24 h. Dried films (surface area of 28.27 cm^2 with an average thickness of 61.4 ± 0.7 μm) were then peeled off the plate and, before analyses, stored for 2 weeks in a desiccator containing silica gel.

3.2.2. Paper II

Three different batches of films were prepared for the release tests: 1) MFC films including lysozyme (1g/10g MFC), coded as M-L10; 2) M-L10, also including glycerol (0.4g/10g MFC), coded as M-L10-G4; M-L10 also including NaCl (1g/10g MFC), coded as M-L10-N10. For all the above formulations, an initial 0.89% water dispersion of MFC was used. Before incorporation in the polymer matrix, the lysozyme powder was firstly dissolved in cold water at room temperature for 2 hours. When necessary, the third component (i.e. glycerol or NaCl) was added as the last step of the preparation of the water dispersion, which was then left to settle for 2 hours. At this point, a known amount of the antimicrobial water dispersion was poured into Petri dishes (∅ 8.5 cm) to obtain a final film weight of ~20g/m^2. Before the release experiments, samples, in the form of 5×2 cm^2 strips, were stored in a climatic chamber (23°C and 50% RH) for one week.

3.3 Analytical Methods and Instruments

3.3.1 Paper I

3.3.1.1 Moisture measurements

Residual moisture of the coatings after drying was measured by means of a halogen moisture analyzer, mod. HG63 (Mettler Toledo, Zurich, Switzerland).

3.3.1.2 Thickness measurements

The thickness of the dry films was measured using a micrometer (Dialmatic DDI030M, Bowers Metrology, Bradford, UK) to the nearest 0.001 mm at 10 different random locations. Unless otherwise specified, all data shown are the average of five replicates.

3.3.1.3 Dye release kinetics

Dye-loaded PVOH films were put into flasks containing 50 mL of a hydro-alcoholic solution (water/ethanol = 1/9) as the releasing medium. This mixture allowed monitoring of the dye release over an extended temporal window without dissolution of the physically cross-linked PVOH network, owing to the non-solvent feature of ethanol toward this polymer [Fuchs, 1989]. The dye release experiments were conducted by keeping the flasks at 20°C under moderate shaking (100 rpm) using a Flask Dancer 270292 orbital shaker (Boekel Scientific, Feasterville, PA, USA). The dye release kinetics were built by assessing the dye concentration in the hydro-alcoholic solution over a time span of 47,700 min (i.e. ~33 days). Absorption of the dye at 610 nm was recorded at different time intervals using a Lambda 650 UV/VIS spectrophotometer (PerkinElmer, Waltham, MA, USA). The absorbance values were then converted into concentration values by the calibration curve, which was obtained by means of standard solutions (three replicates) from 1 ppm to 100 ppm (mg/kg). Each data point of the release curves represents the mean of nine replicates. The swelling ratio (SR) was calculated on a second set of PVOH films according to the following formula:

$$SR(\%) = \frac{w_w - w_d}{w_w} \qquad (1)$$

where Ww and Wd are the wet and dry weight (g) of the PVOH films, respectively. Since it was not possible to handle the samples 4-88 and 40-88 after 13 days soaking in the water/ethanol solutions, swelling evolution was no longer monitored after 13 days.

3.3.1.4 X-ray diffraction (XRD)

The X-ray diffraction patterns of the films were obtained using a Rigaku DMAX-II diffractometer (Rigaku Corporation, Tokyo, Japan) with graphite-monochromatized Cu-K_ radiation (1.5406Å) and a generator operating at 40 kV and 40 mA, under the following conditions: step width 0.02°; time per step 2 s; divergence slit 1.0°; soller slit 1.0°; antiscatter slit 0.15°.

3.3.1.5 Differential scanning calorimetry (DSC)

The thermal properties of the PVOH samples were determined by differential scanning calorimetry (DSC) analysis using a DSC 1 (Mettler Toledo, Columbus, OH, USA) supplied with a quench-cooling accessory and a GC 100 gas controller. Before measurements, the instrument was calibrated with the well-characterized standard indium, which has a heat of fusion (ΔH) of 28.4 J g^{-1} and a melting temperature (Tm) of 156.6°C. Approximately 5 mg PVOH samples were then put in a hermetically sealed aluminum pan (40 μL) to prevent any loss of moisture during the experiment. An initial scan from 25°C to 250°C was followed by an isothermal step (250°C for 5 min), with the goal of better determining the crystallization temperature. Samples were then cooled to 25°C. The second heating scan was carried out from 25°C to 250°C. All scans were performed in an inert environment (50 mL min^{-1} N_2) at a rate of 10°C min^{-1}. The glass transition temperature (Tg) was calculated as the midpoint of the inflexion in the baseline (second heating scan) caused by the discontinuity of the specific heat capacity of the sample. The melting temperature (Tm) was set at the endothermic peak, which was also used to calculate the degree of crystallinity according to the following formula, assuming a linear relationship between the peak area and crystallinity [Peppas and Merrill, 1976]:

$$Xc(\%) = \frac{\Delta H}{\Delta H_{100}} \times 100 \qquad (2)$$

where Xc is the crystallinity of the semi-crystalline polymer, ΔH the experimental heat of fusion (J g^{-1}) and ΔH_{100} the heat of fusion of the 100% crystalline material (equal to 138.6 J g^{-1} for PVOH). All the above parameters were calculated by the software Star^e version 9.20 (Mettler Toledo, Columbus, OH, USA). Three replicates were used for each of the three PVOH films.

3.3.1.6 Field-emission scanning electron microscopy (FE-SEM)

Cross-sections and surfaces of PVOH films were examined using a Hitachi S-4800 FE-SEM (Schaumburg, IL, USA) in order to acquire information on the overall physical organization of the polymer network. Surface test specimens were mounted with carbon tape on stubs. Cross-sectioned samples were cut into thin pieces with a scalpel and mounted on a Hitachi thin specimen split mount holder, M4 (prod. No. 15335-4) to observe the cross-section. Before insertion into the microscope, samples were sputter coated with gold to a thickness of approximately 10 nm (to avoid charging the samples), using an Agar High Resolution Sputter Coater (model 208RH), equipped with a gold target/Agar thickness monitor controller.

3.3.1.7 Statistical analysis

Statgraphics Plus 4.0 software (STSC, Rockville, USA) was used for the one-way ANOVA to check for differences between samples. The mean values, when appropriate, were separated by the LSD multiple range test at $p < 0.05$. The dye kinetic release curves were obtained by fitting the analytical solution of Fick's second law for a planar sheet to the experimental data solved using Matlab® (The Mathworks Inc., Natick, MA, USA).

3.3.2 Paper II

3.3.2.1 Thickness measurements

The thickness of samples was measured at ten different random positions on each sample, using a digital micrometer (Micrometer 51 Lorentzen & Wettre, Stockholm, Sweden).

3.3.2.2 Lysozyme release kinetics

Lysozyme-loaded MFC films were put into flasks containing two different contact media (50 mL), namely distilled water and water/ethanol 10 wt.% solution, which are two food simulants (simulant A and simulant C, respectively) within the food contact material

legislation [Commission Regulation (EU)]. The lysozyme release experiments were conducted over a time span of 10 days (after which the release from the MFC films was no longer observed) by keeping the flasks at 6°C and 20°C under moderate shaking (100 rpm) using a Flask Dancer 270292 orbital shaker from Boekel Scientific (Feasterville, PA, USA). The release kinetics were built by assessing the lysozyme concentration in the simulant at different time intervals, by recording the absorption at 280 nm [Mascheroni *et al*., 2010] using a Lambda 650 UV/VIS spectrophotometer (PerkinElmer, Waltham, MA, USA). The absorbance values were then converted into concentration values by the calibration curve, which was obtained by means of standard solutions (three replicates) from 50 ppm to 250 ppm (mg/kg). Each data point of the release curves represents the mean of nine replicates.

3.3.2.3 Conductometric titration

Charge density of MFC was determined by conductometric titration according to the method described in a previous work [Farris *et al*., 2012]. Briefly, a MFC aqueous dispersion (0.1 wt %) was first treated with an excess (15 mL) of 0.1 N hydrochloric acid (HCl), to completely neutralize the negative charge possibly distributed along the cellulose backbone. Conductometric titration was performed by adding 0.1 N sodium hydroxide (NaOH) under gentle stirring (100 rpm). Ionic conductivity was evaluated after sequential injections of 0.1 mL drops of NaOH at 0.40 μL s^{-1}. As the conductance decreased and the first equivalence point was approached, drops of 0.05 mL at 0.15 μL s^{-1} flow rate were dispensed, while the initial set up conditions were brought backbeyond the "constant-conductivity" region. The titrant was added approximately every 60 s, to allow sufficient time for equilibrium to be reached between readings. pH was continuously measured simultaneously. Finally, the charge density (mmol g^{-1}) was quantified by a graphical method, i.e. plotting the measured ionic conductivity versus total titrant and calculating the volume (mL) of titrant required to fully deprotonate all charged groups on cellulose from the intersection points of the linear segments of the ionic conductivity plot before and after the equivalent point (or breakpoint).

3.3.2.4 Electron microscopy analyses

Cross-sections and surfaces of MFC films were examined using a Leo1430 scanning electron microscopy (Zeiss, Oberkochen, Germany) in order to acquire information on the overall physical organization of the polymer network. Surface test specimens were mounted with

carbon tape on stubs. Cross-sectioned samples were cut into thin pieces with a scalpel and mounted on a thin specimen split mount holder to observe the cross-section. Before insertion into the microscope, samples were sputter coated with gold to a thickness of approximately 10 nm (to avoid charging the samples), using an Agar High Resolution Sputter Coater (model 208RH), equipped with a gold target/Agar thickness monitor controller.

Transmission electron microscopy (TEM) images were captured to visualize the MFC fibrils dimension. To this purpose, 5 µL of a 0.1 wt.% water dispersion was deposited onto a Formvar-coated Cu grid (400 mesh). Observations were made after 24 hours (i.e., the time required to allow solvent evaporation) using an LEO 912 AB energy-filtering transmission electron microscope (EFTEM) (Carl Zeiss, Oberkochen, Germany) operating at 80 kV. Digital images were recorded with a ProScan 1K Slow-Scan CCD camera (Proscan, Scheuring, Germany).

3.3.2.5 Laser profilometry analysis

Laser profilometry tests were also conducted to check for any potential influence of lysozyme, glycerol, and NaCl on the surface morphology of the MFC films. Samples of approximately 1×1 cm^2 were mounted on an object glass with double-sided tape. The samples were covered with a layer of gold before image acquisition. Ten areas were acquired from each film. The size of the topography images was 1×1 mm^2, with a resolution of 1 µm/pixel. The analysis was performed with the SurfCharJ plugin. Lateral structures larger than 40 µm were suppressed.

3.3.2.6 Statistical Analysis.

Statistical significance of differences in the release and surface properties of films was determined by one-wayanalysis of variance (ANOVA), using JMP 5.0.1 software (SAS, Cary, NC). The mean values, where appropriate, were compared by Student's *t*-test with a significance level (p) < 0.05. The lysozyme kinetic release curves were obtained by fitting the analytical solution of Fick's second law for a planar sheet to the experimental data solved using Matlab® (The Mathworks Inc., Natick, MA, USA).

4 RESULTS AND DISCUSSION

4.1 Paper I

4.1.1 Dye release kinetics

The ethanol-rich solvent mixture used in this work made it possible to preserve the integrity of the PVOH films over 33 days of monitoring; no secondary effect (e.g. dissolution, crazing, wrinkling, or breakage) besides swelling occurred macroscopically on the PVOH samples during the release experiments. Therefore, it can be reasonably assumed that the release took place from a planar sheet throughout the entire time span of analysis. Generally, the overall release process of low molecular weight compounds from strongly hydrophylic networks (such as PVOH) can be conceived as the result of three phenomena: (i) solvent diffusion into the film network; (ii) relaxation of the polymer matrix, owing to the swelling of the strongly hydrophilic PVOH molecules; (iii) diffusion of the active compound from the swollen polymeric network into the surrounding medium. Due to both the complexity of simultaneous monitoring of the abovementioned phenomena and the presence of ethanol, it has been demonstrated as expedient to model the experimental release data by a simple approach under the following assumptions [Mastromatteo *et al.*, 2009]: (1) both water diffusion and relaxation of molecular chains are faster than the diffusion of the low molecular weight compound through the slightly swollen network, (2) the increase in film size due to swelling is negligible, and (3) dye diffusion takes place in an homogeneous and symmetric medium. Moreover, the volume of the liquid medium has been considered infinite and it has been assumed that the external mass transfer coefficient at the solid-liquid interface is negligible. The solution of Ficks second law for a planar sheet with constant boundary conditions can thus be used [Langer and Peppas, 1983]:

$$M_t = M_\infty \left\{ 1 - \frac{8}{\pi^2} \sum_{n=0}^{n-\infty} \frac{1}{(2n+1)^2} \exp\left[-\frac{D_{dye}}{l^2} (2n+1)^2 \pi^2 t \right] \right\} \qquad (3)$$

where M_t represents the amount (mg/kg) of the diffusing compound released at time t (s); M_∞ is the corresponding amount at infinite time (i.e. at the equilibrium), taken as the initial quantity loaded in the film; D_{dye} is the dye apparent diffusion coefficient (cm^2/s) through the

polymeric matrix, l is the thickness (cm) of dry films. The release kinetics were obtained plotting the M_t/M_∞ ratio versus the square root of time, in order to elucidate the diffusion behavior of the low molecular weight molecule according to the classification proposed by Crank [Crank, 1975]. Fig. 6a displays the experimental release data. The final amount of dye released from samples 4-88, 40-88, and 10-98 after 33 days accounted for, respectively, 60%, 45%, and 10% of the initial amount loaded in the films. Besides physicochemical considerations, which will be discussed shortly, newly established weak interactions (e.g. ion-dipole forces) between the negatively charged dye and the polar pendant hydroxyl groups along the PVOH backbone could have contributed in thwarting the diffusion process of the small molecule dye. Although this conclusion cannot be directly induced from our data, the different affinity of the dye for the polymer matrix can be deduced by the partition coefficients calculated for each film at infinite time according to the following formula:

$$K = \frac{C_{polymer,\infty}}{C_{solvent,\infty}} \qquad (4)$$

where $C_{polymer,\infty}$ and $C_{solvent,\infty}$ are, respectively, the migrant concentration (mg/kg) in the polymer and in the liquid medium at the equilibrium. The resulting K values are reported in Table 2. Since this coefficient compares the relative affinity of the migrant between polymer and solvent, the following classification accounting for the affinity of the three PVOH films for the dye can be gathered: 10-98 > 40-88 > 4-88, which confirms the previous hypothesis of an increased number of interactions for the OH richest PVOH films.

Another striking feature is that all samples showed an initial “induction” or “lag” phase, here intended as the time required before the release process set off (see the inset of Figure 6a). A plausible explanation for the appearance of such ‘no-release’ lapse can be the simultaneous presence of both a non-solvent (ethanol) and a solvent (water) in contact with the polymer matrix. Water-ethanol interactions modify the availability of water molecules toward the polymer matrix, thus slowing down the relaxation of the polymer chains [Morita *et al.*, 2000]. This is also confirmed by the swelling ratio values collected during the induction phase (Figure 7a). These values are noticeably lower than those otherwise obtained from uncrosslinked and cross-linked PVOH samples immersed in a 100% water solution at room temperature during a time span of similar magnitude [Buonocore *et al.*, 2003]. Figure 6b

displays the fitting of the mathematical model expressed by Eq. (3) to the experimental data. This procedure allowed for estimating the apparent diffusion coefficient (D) of the released dye molecules for all three PVOH films. Due to the hypotheses made for deriving Eq. (3), D has to be considered with any thermodynamic meaning. For this reason, it can be more useful to consider the ratio D/l^2 since it is directly related to the dye release rate from the film to the outer hydro-alcoholic solution [Mastromatteo *et al.*, 2009]. The D_1/l^2 values can be easily inferred from Table 2. This ratio was greatly decreased for sample 10-98 ($3.68 \times 10{-}7\ s^{-1}$) compared to samples 40-88 ($2.02 \times 10{-}6\ s^{-1}$) and 4-88 ($2.05 \times 10{-}6\ s^{-1}$). Eq. (3) was also fit to the experimental data underlying the sudden jump observable in the dye release evolution (see arrow in Figure 6b). The appearance of the film burst, already reported for PVOH-based release systems [Morita *et al.*, 2000], can be reasonably attributed to the partial collapse of the amorphous phase, which ultimately produced an increase in the total amount of the dye molecule released into the surrounding medium. It was possible to associate a second diffusion coefficient (D_2) for all the three PVOH samples (Table 2) by a new independent procedure that took into account new and different starting points (t_1, t_2, and t_3 for PVOH samples 40-88, 10-98, and 4-88, respectively, see Figure 6b). The D_2/l^2 values were significantly lower for sample 40-88 ($1.42 \times 10{-}7\ s^{-1}$) compared to samples 10-98 and 4-88 ($6.31 \times 10{-}7\ s^{-1}$ and $6.15 \times 10{-}7\ s^{-1}$, respectively), presumably due to the higher molecular weight, i.e. higher degree of molecular chain entanglement. Eventually, the three PVOH samples, although released a different amount of dye as clearly depicted in Figure 8, had in common a similar release profile characterized by a lag-phase followed by a first rapid release step and a second release burst. As anticipated, the release patterns disclosed by the PVOH films will be now discussed on the basis of physical aspects intimately linked to the chemical structure of the three PVOH matrices.

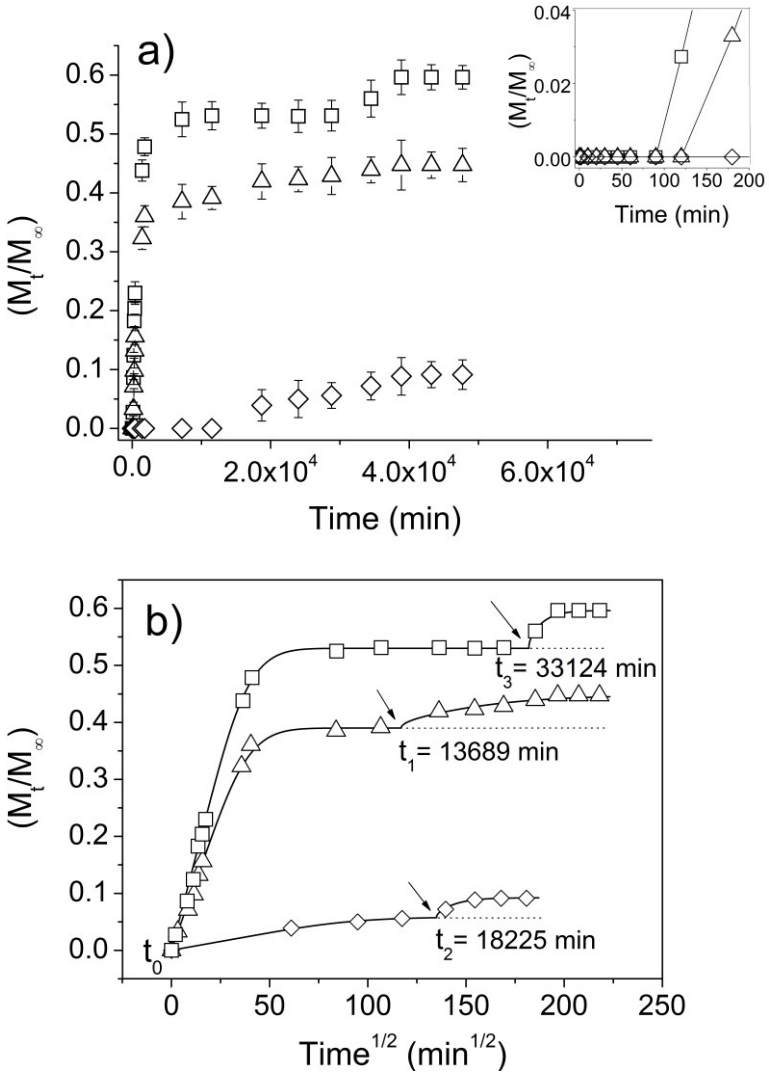

Figure 6. Original (a) and back-shifted experimental (symbols) and calculated (line) release data (b) of the Coomassie brilliant blue dye at 20°C from the 4-88 (□), 40-88 (△), and 10-98 (◇) PVOH film samples.

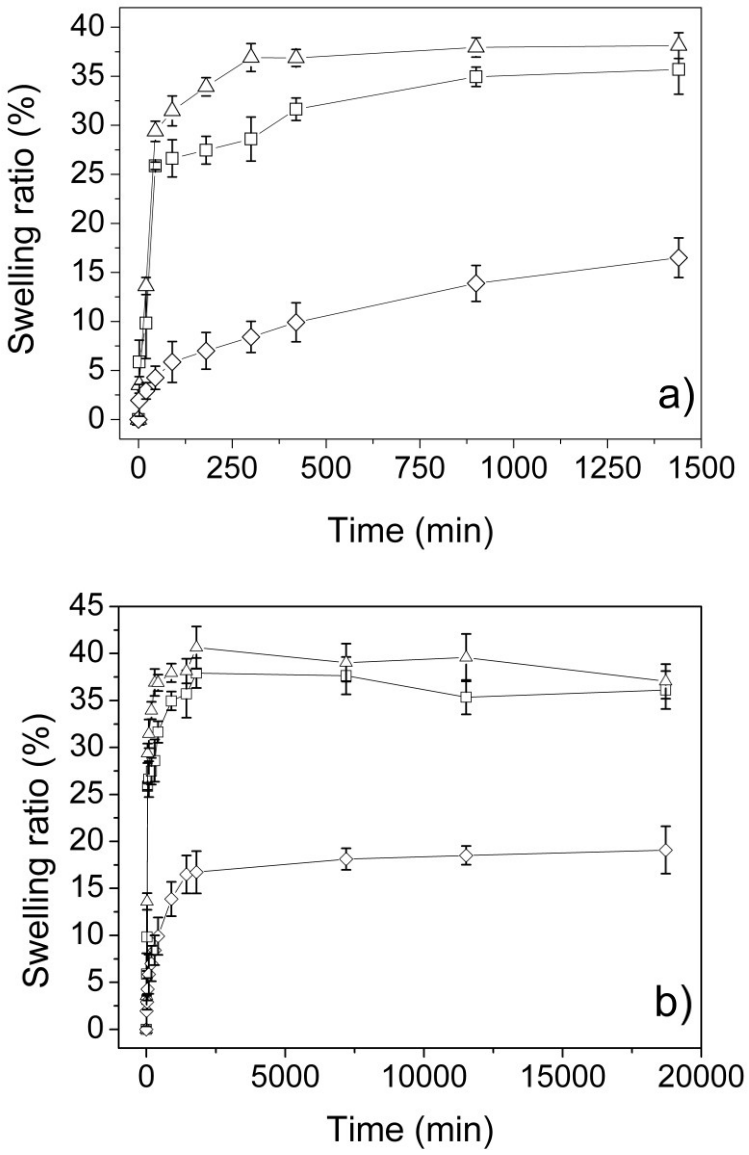

Figure 7. Swelling ratio evolution of PVOH samples 4-88 (□), 40-88 (△), and 10-98 (◇) during the first 24 hours of the release experiment (a) and after 13 days (b).

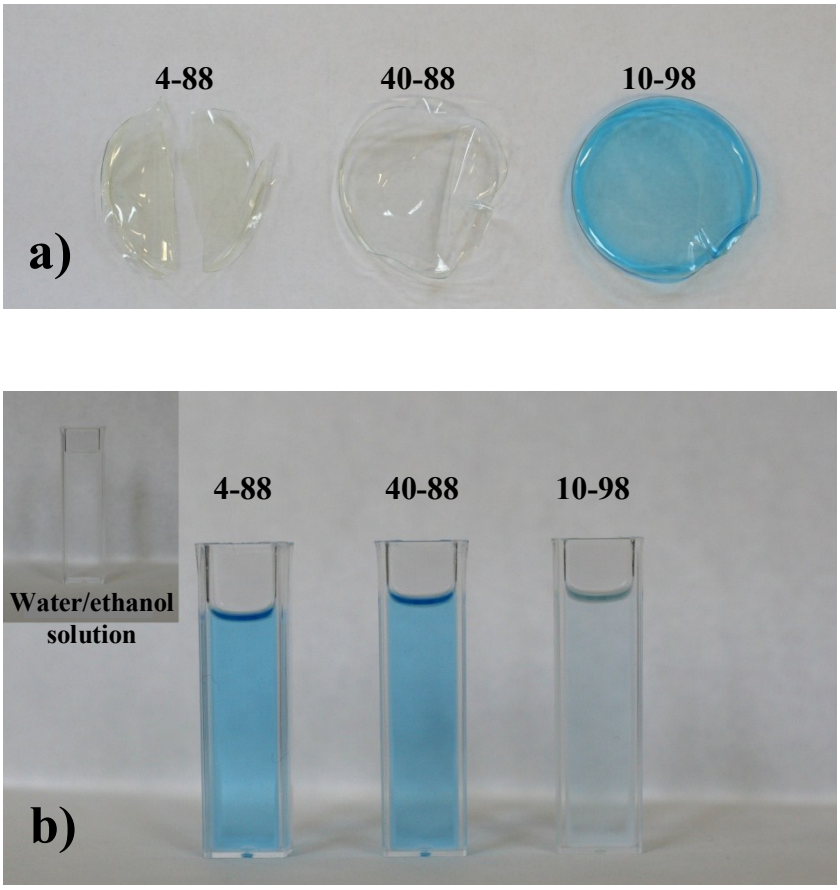

Figure 8. Samples (a) as appeared after 33 days immersion in the water/ethanol solution and water/ethanol solution (b) after dye release [above left the hydro-alcoholic solution before release].

PVOH type	Dry weight (g)	Moisture content (%)	l (μm)	K	D_1 (cm^2/s)	D_2 (cm^2/s)
4-88	$0.27^{a} \pm 0.011$	$1.80^{cd} \pm 0.52$	$63.75^{ef} \pm 6.28$	0.68 ± 0.08^{g}	$8.33E\text{-}11^{l}$	$2.50E\text{-}11^{n}$
40-88	$0.26^{b} \pm 0.004$	$1.12^{c} \pm 0.41$	$64.17^{e} \pm 0.88$	1.24 ± 0.14^{h}	$8.33E\text{-}11^{l}$	$5.83E\text{-}12^{o}$
10-98	$0.26^{ab} \pm 0.002$	$1.93^{d} \pm 0.41$	$56.33^{f} \pm 5.01$	9.95 ± 0.96^{i}	$1.16E\text{-}11^{m}$	$2.00E\text{-}11^{n}$

Different superscripts within a group (i.e. within each parameter) denote a statistically significant difference ($p < 0.05$).

Table 2. Dry weight, moisture content, thickness (l), partition coefficient PVOH/solvent (K), and diffusion coefficients (D_1 and D_2) of the dye-loaded PVOH films.

4.1.2 XRD analysis

Figure 9 shows the XRD patterns for the three different PVOH films tested in this work, while the main parameters drawn from the diffractograms are reported in Table 3. All the three samples exhibited one strong peak at 2θ ~19° and a second weaker peak at 2θ ~40.5°. The latter has been attributed to the (2 2 0) reflection [Bunn, 1948], whereas the former peak has been already reported to correspond to a typical doublet reflection of (1 0 1) and (1 0 −1) planes of the semicrystalline atactic PVOH containing the extended planar zigzag chain conformation [Kim *et al.*, 2008; Assender and Windle, 1998]. However, this peak was gradually shifted to lower diffraction angles from sample 4-88 to sample 10-98, with sample 40-88 in between. Shifting toward lower angles is generally correlated to an increase in periodicity of the crystalline structure, implying an increase in the size of the PVOH crystallites [Kim *et al.*], in agreement with the results obtained by applying the Scherrer equation for the estimation of the size (thickness, $Ð_{hkl}$) of the crystallites:

$$D = \frac{K_\gamma}{\beta \cos \vartheta} \qquad (5)$$

where K is the Scherrer shape factor near unity (here set at the value of 0.94), λ is the wavelength of the X-ray, β is the breadth (in radians, at half the peak value) of the diffraction

peak associated with the (h k l) planes, and θ the diffraction angle (in radians) [Gedde, 1995]. Data on the crystallite dimensions, reported in Table 3, are indicative of the fact that the crystallite domains in sample 10-98 were larger compared to those in samples 40-88 and 4-88, the latter sample apparently having the smallest crystallite size. Concurrently, the diffraction peak related to sample 10-98 became narrower and sharper compared to the other two peaks, suggesting more closely packed crystallites with fewer imperfections [Poursamar *et al*., 2011; Doppers *et al*., 2004]. According to the release data illustrated in the previous section, both the degree of crystallinity and the crystal organization apparently played an important role in the diffusion kinetics of the dye molecules into the hydro-alcoholic medium. The different degree of crystallinity seems to justify the extended induction phase observed for the sample 10-98 (~8 days compared to ~1.5 h and ~2 h for samples 4-88 and 40-88, respectively), as the higher amount of crystallite regions could have induced a decrease in the relaxation rate of the polymer chains (the only phase available for water uptake is the amorphous one). Therefore, the presence of the crystal phase in the film would have a similar effect as chemical crosslinking in amorphous polymers [Tanigami *et al*., 1995]. In addition, the total release of dye decreased proportionally to the degree of crystallinity, most likely due to the physical impedance offered by the crystal regions to the diffusion of the dye. The D_1/l^2 values calculated for the three PVOH films are consistent with the generally accepted rule that D decreases with an increase in crystallinity, basically due to an increase in both the tortuosity factor (linked to the physical obstacles represented by the crystallite regions) and the chain-immobilization factor (linked to the restriction of chain movement in the amorphous phase). We also believe that part of the dye loaded in the PVOH water solutions got entrapped during the formation of the crystalline domains (i.e. during the drying process) and there was retained throughout the release experiment duration, as suggested by the total amount of the dye released after 33 days, which never reached the theoretical 100%. According to this hypothesis, the work of Mallapragada and Peppas (1997) demonstrated that the drug release from semicrystalline polymers physically crosslinked (such as the PVOH films used in this work) is controlled by the rate of crystals dissolution in a solvent, i.e. the total release could never be achieved as long as the crystal phase is not completely dissolved. This observation indicates that the crystalline phase of the PVOH films used in this work was not dissolved upon contact with the hydro-alcoholic medium. This was also corroborated by the swelling ratio data. Samples soaked in the hydro-alcoholic medium never experienced abrupt

volumetric expansion, and the swelling ratio values after 13 days (Figure 7b) were well below the range 200-500% observed for both PVOH films of different DH immersed in pure water [Morita *et al*., 2000] and PVOH films immersed in several mixed solvents of dimethylsulfoxide (DMSO) and water with different solvent compositions [Tanigami *et al*., 1995] after the same time span. In addition, samples 10-98, 40-88 and 4-88 did not dissolve in the medium after 33 days, while the same samples in direct contact with pure water dissolved completely, as demonstrated by our preliminary experiments (data not shown). This is in agreement with previous results that suggest the complete disruption of the crystalline domains of untreated PVOH films, i.e. subjected to neither annealing [Assender and Windle, 1998] nor freezing-thawing [Hassan and Peppas, 2000]. Since the polymer will not dissolve until the crystal structure is broken down [Assender and Windle, 1998], the original crystalline pattern of the three PVOH samples is thought to have not been greatly affected by the water molecules. This was also demonstrated by Sakurada *et al*. [Sakurada *et al*., 1955], who analyzed the crystallinity of swollen PVOH films, showing that swelling does not change ('melt out') the crystalline regions of the PVOH matrix. However, it has been pointed out that the average size of the crystallite, its size distribution and the packing order of molecules in crystallites are variable factors within the total crystallinity and some of the smaller crystals or with a lower degree of packing order might have experienced partial dissolution on swelling [Tanigami *et al*., 1995]. Therefore, based on the above considerations, while we can assume with a degree of certainty that the crystallinity (x_c) of sample 10-98 did not change significantly after contact with the water/ethanol medium, the x_c values of samples 40-88 and 4-88 might have slightly decreased during swelling.

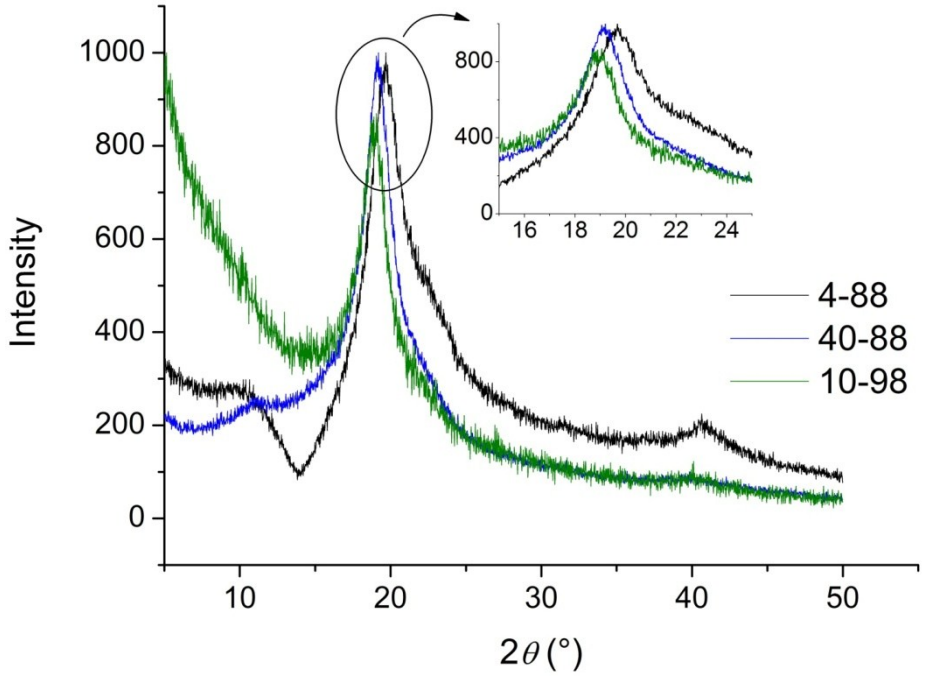

Figure 9. XRD traces of the 4-88, 40-88, and 10-98 PVOH films.

PVOH type	Diffraction peak (2θ)	Peak intensity	Peak area	Crystallite size (nm)
4-88	19.68	1000	4727.61	2.30
40-88	19.20	1000	2802.89	3.53
10-98	19.06	869.24	1656.35	4.04

Table 3. Main parameters obtained from the XRD traces of the different PVOH films.

4.1.3 DSC analysis

DSC traces (Figure 10) display the differences between the samples as far as their thermal properties are concerned. The thermal parameters drawn from the DSC analysis are summarized in Table 4. The difference in T_g between sample 4-88 and sample 40-88 can be explained by Flory's theory, according to which the glass transition temperature decreases with decreasing molecular weight due to an increased segmental mobility of the polymer chains [Fox and Flory, 1950]. The highest T_g observed for sample 10-98 accounts for the high packing efficiency of the planar zigzag conformation [Martien, 1986]. The effect of the crystal phase on the mobility of the amorphous molecules must also be mentioned, since the tension of the amorphous molecules should be enhanced by the formation of the crystallites [Tanigami *et al*., 1995]. The melting temperatures recorded reflected the capability of the polymer chains to arrange into ordered domains. This is believed to be enhanced by the small size of the hydroxyl groups, which allows the chains to adopt a planar zigzag conformation under the action of hydrogen bonding between the pendant hydroxyl groups along the molecule [Hodge *et al*. I, 1996; Hodge *et al*. II, 1996]. Although no statistically significant difference was detected between samples 4-88 and 40-88 concerning the T_m, the former sample showed a higher tendency to form crystal regions, which was also confirmed by the observed trend in the degree of crystallinity. Presumably, this might be due to the higher molecular weight of sample 40-88, which could have hindered the re-organization of the molecular chains into ordered domains upon cooling, thus favoring the growth of the amorphous phase. This was also confirmed by the swelling ratio evolution reported in Figure 7a: the higher solvent uptake by sample 40-88 during the first 24 h could be linked to a larger amorphous phase compared to sample 4-88. Both T_m and crystallinity increased dramatically for sample 10-98, in line with the values reported in the literature for highly hydrolyzed atactic PVOH polymers [Tanigami *et al*., 1995] and in agreement with the XRD data. This indisputably confirms the enhanced tendency of sample 10-98 to generate crystal domains, probably due to the synergistic effect of both a high hydrolysis degree and a low molecular weight. The huge difference in thermal properties between the low DH samples (4-88 and 40-88) and the sample 10-98 gives reason for the observed release patterns. It is well established that the region of the polymer in which water molecules can be taken up is only the amorphous phase of PVOH. As a consequence of water absorption, the mobility of the polymer chains in the amorphous region will increase, with a concomitant shift of the T_g

toward lower temperatures due to the plasticizing effect of water [Assender and Windle, 1998; Finch, 1973], which causes the polymer to undergo a glass to rubber transition [Thomas and Windle, 1980]. Lowering of the T_g results in the relaxation of the network chains, which is macroscopically accompanied by the swelling of the matrix. As mentioned before, this is restrained by high degree of crystallinity, as in the case of sample 10-98. Therefore, it can be said that the lower amount of dye released from sample 10-98 must be related to the decreased diffusion of the penetrant (water) and the decreased relaxation of the polymer chains compared to samples 40-88 and 4-88, which in turn exhibited an increased swelling behavior.

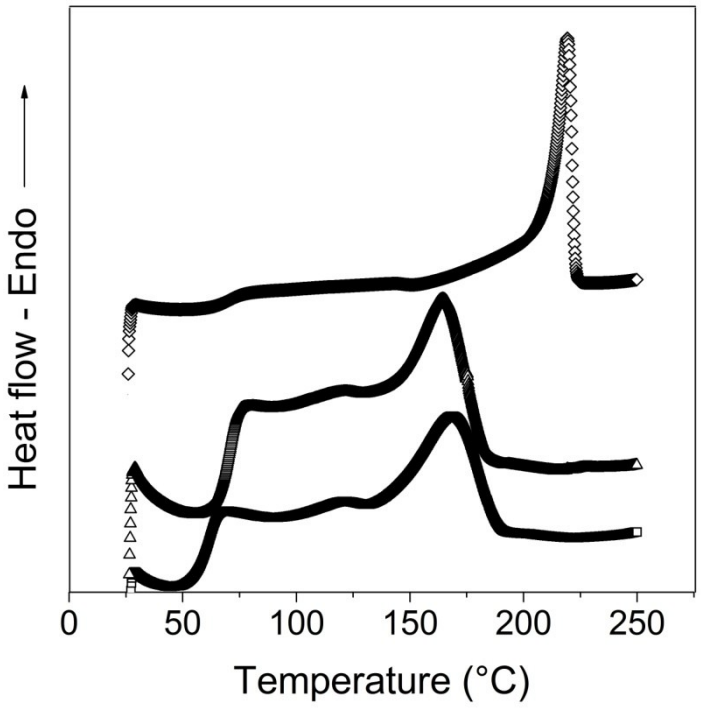

Figure 10. Representative DSC traces (second heating scan) of the 4-88 (□), 40-88 (△), and 10-98 (◇) dried PVOH samples.

PVOH type	T_g (°C)	T_m (°C)	x_c (%)
4-88	60.14 (± 0.54)[a]	170.21 (± 1.35)[c]	15.98 (± 1.24)[e]
40-88	66.94 (± 3.38)[b]	168.12 (± 2.51)[c]	13.62 (± 1.71)[e]
10-98	71.77 (± 3.43)[b]	219.55 (± 0.75)[d]	50.96(± 2.13)[f]

Different superscripts within a group (i.e. within each parameter) denote a statistically significant difference ($p < 0.05$).

Table 4. Glass transition temperature (T_g), melting temperature (T_m), and crystallinity degree (x_c) obtained from the DSC traces of the different PVOH films.

4.1.4 Films morphology

Samples of similar thickness, weight and dry matter (Table 3) were used to obtain the cross-section SEM images at two different magnifications (20k× and 40k×) shown in Figure 11, which highlight the global morphology of the polymer network. Sample 4-88 exhibited a spiky "stalactite-like" morphology (20k× magnification), with an apparently high degree of interstices and empty spaces within the molecular chain network (40k× magnification). The overall morphology changed dramatically for the sample 40-88, i.e. with increased molecular weight. This sample showed an apparently rougher morphology, with an "orange peel-like" texture (20k× magnification) due to molecular aggregates seemingly oriented parallel to the longitudinal direction (40k× magnification). Finally, sample 10-98 displayed a more compact and tighter structure (20k× magnification), presumably with very limited free volume between polymer chains (40k× magnification). Although SEM images cannot provide direct information on molecular mechanisms, the different morphologies observed for the three PVOH samples can be tentatively linked to the physicochemical heterogeneity of the polymer matrices, i.e. in terms of molecular weight and degree of hydrolysis. On one hand, apparently aggregated morphologies (e.g. sample 40-88) can be due to extensive molecular folding and entanglements, which are well known to increase proportionally with the molecular weight. On the other hand, denser structures (e.g. sample 10-98) are probably induced by higher degree of hydrolysis because of the increased intramolecular and intermolecular cohesive energy of the polymer, mainly driven by extensive hydrogen bonding between the hydroxyl groups along the polymer backbone. At the same time, the low molecular weight of sample 10-98 might have promoted the establishment of intermolecular hydrogen bonds due to high chain mobility. These considerations are in agreement with both the XRD and DSC data previously discussed. In particular, the structural change from the packed lamellar structure of sample 10-98 to the fibril-like and disordered structures of samples 40-88 and 4-88, respectively, appeared to be linked to broadening of the XRD peak area, which involves a depression of crystallinity. Observations arising from the SEM analysis suggest that the release profile of the molecule dye from the PVOH matrices can be somehow influenced by different morphologies (presumably linked to different molecular arrangements), which in turn can be induced by a proper selection of the polymer matrix.

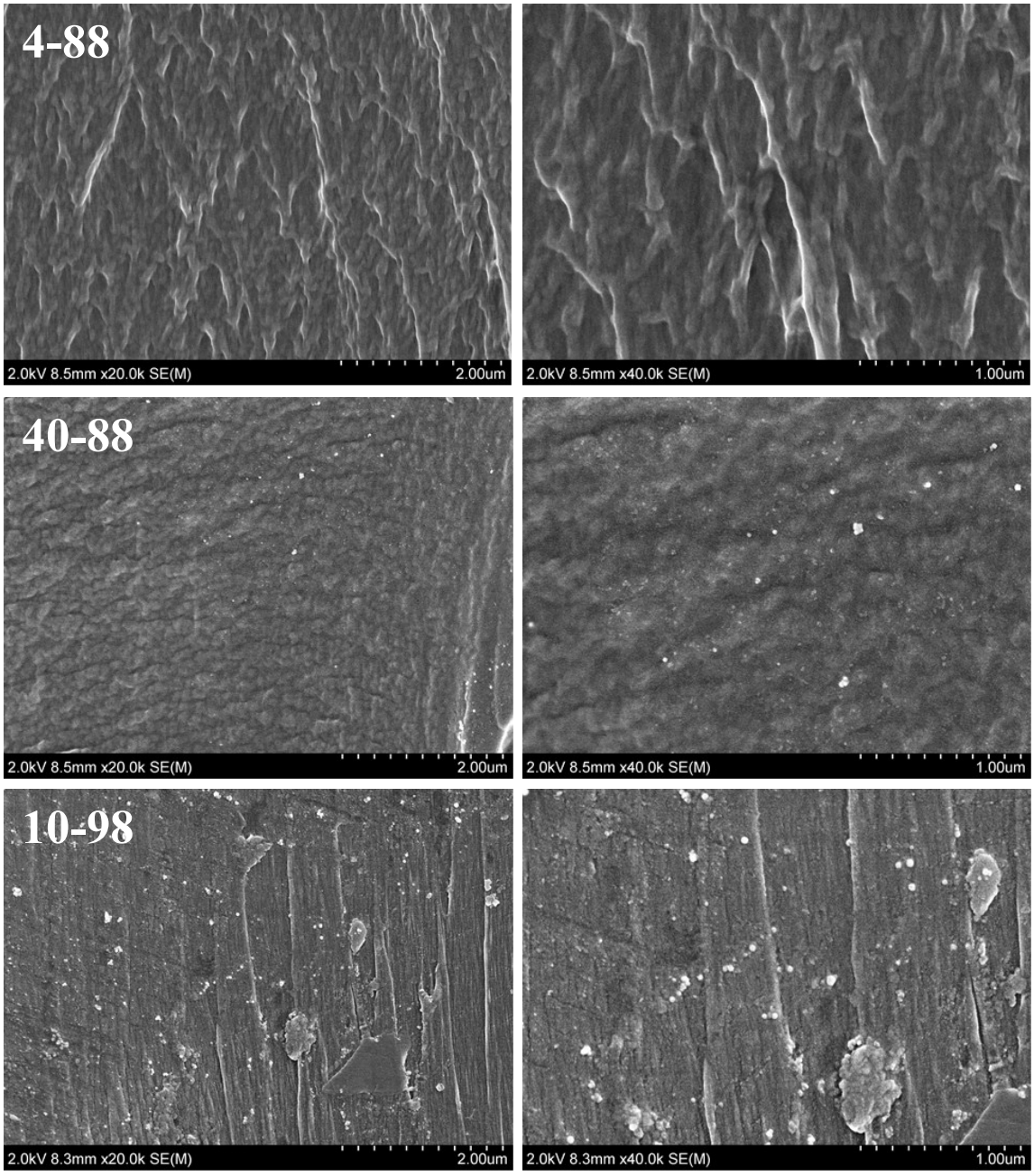

Figure 11. Cross-sectional SEM images (20k×, left column; 40k×, right column) of the three PVOH films. Images in the same row are from the same sample.

4.1.5 Effect of the solvent composition

The effect of the hydro-alcoholic solution in contact with the PVOH matrices cannot be neglected in the discussion of the aforementioned results. Mixing water with another solvent at various ratios is a well-established practice to modulate the solubility of hydrophilic polymers such as PVOH. In particular, with respect to the development of controlled release systems, the solvent composition becomes an important factor to control the swelling behavior of the polymer. The water/ethanol mixing ratio used in this work (1/9) allowed monitoring the release of the dye from all the three PVOH films, without dissolution of the films being observed over the entire duration of the experiments. The same results would have been otherwise unattainable with both ethanol richer solutions and water richer solution, due to a too low and too high relaxation of the polymer matrix, respectively. In other words, the presence of ethanol in the mixture made possible to tune the release rate by controlling the relaxation of the polymer chains to the extent that both fast relaxation and very slow relaxation were avoided. This is thought to be due to the different local affinity of the two solvents toward PVOH, the water molecules having higher affinity. Therefore, it can be said that ethanol somehow counterbalanced the effect of water molecules on the PVOH physical properties, e.g. ethanol hindered crystallites dissolution and other macroscopic phenomena such as crazing, waving and abrupt increase of swelling followed by catastrophic expansion of the swollen film, which are typical of water-rich solvents.

4.2 Paper II

4.2.1 Lysozyme release kinetics

The overall release process of low molecular weight compounds (e.g. lysozyme) from strongly hydrophylic networks (such as MFC) can be conceived as the result of three phenomena: i) solvent diffusion into the film network; ii) relaxation of the polymer matrix, owing to the swelling of the strongly hydrophilic MFC molecules; iii) diffusion of the active compound from the swollen polymeric network into the surrounding medium. The experimental release data were modeled assuming that: 1) both water diffusion and relaxation of molecular chains are faster than the diffusion of the low molecular weight antimicrobial compound through the swollen network; 2) lysozyme diffusion takes place in an homogeneous and symmetric medium; 3) the volume of the liquid medium is infinite and 4) the external mass transfer coefficient at the solid-liquid interface is negligible. Moreover,

modeling of the experimental data only concerned the first diffusion part of the release curve for all samples, i.e. the time span between the beginning of the experiments (t = 0) and the first steady state level. Any possible secondary diffusion process, associated with a sudden jump in the release curve, was not considered for further mathematical data treatment. The solution of Fick's second law for a planar sheet with constant boundary conditions can thus be used [Crank, 1975]:

$$M_t = M_\infty \left\{ 1 - \frac{8}{\pi^2} \sum_{n=0}^{n-\infty} \frac{1}{(2n+1)^2} \exp\left[-\frac{D_{LYS}}{l^2} (2n+1)^2 \pi^2 t \right] \right\} \qquad (6)$$

where M_t represents the amount (mg/kg) of the diffusing compound released at time t (s); M_∞ is the corresponding amount at infinite time (i.e. at the equilibrium), taken as the initial quantity loaded in the film; D_{LYS} is the lysozyme apparent diffusion coefficient (cm^2/s) through the MFC polymer matrix, l is the thickness (cm) of dry films. The release kinetics were obtained plotting the M_t / M_∞ ratio versus the square root of time, in order to elucidate the diffusion behavior of the low molecular weight antimicrobial molecule according to the classification proposed by Crank [Crank, 1975]. Figures 12-15 display both the experimental and simulated release data for the three film types under different conditions (simulant A and C at 6° and 23°C). As an overall consideration, it can be observed that the total amount of lysozyme released in the medium never reached values as high as 100% over the time span considered in this work. This means that the main goal of the study was satisfactorily achieved, i.e. the initial amount of antimicrobial initially loaded in the polymer films was not preserved within the first time of contact with the surrounding medium. By contrast, it must be noted that the retention capability of the MFC network towards lysozyme was pronounced insomuch as maximum release data accounted for approximately 13% after 10 days of experiment. This finding can be firstly explained considering newly established weak interactions between MFC and lysozyme (chemical aspect). In particular, MFC carries a net negative charge due to carboxylic acid groups owing to both residues of the hemicellulose fraction and oxidation products of the main cellulose skeleton arising from the refining of the raw material [Freudenberg *et al.*, 2007]. As confirmed by our conductometric measurements (see Figure 16), the negative charge amounted to $0.7925 \pm 0.01 mmol g^{-1}$, which is far lower than other negative polyelectrolyte biopolymers such as pectin [Farris *et al.*, 2012]. Therefore,

it is plausible that electrostatic interactions took moderately place between the negatively charged MFC and the positively charged lysozyme. However, also ion-dipole interactions between lysozyme and the polar pendant hydroxyl groups of cellulose could have contributed in limiting the diffusion process of lysozyme through the MFC network [Cozzolino *et al*., 2012]. Not less important, the density of the aforementioned MFC/lysozyme interactions is another important factor in dictating the final release performance of the MFC matrix. This aspect (physical aspect) is intimately linked to the nano-sized features of MFC. As shown in Figure 17a, MFC is made of fibrils 3-100 nm wide and ~10 µm in length, although this strongly relies on the fibrillation procedure, being also possible to produce sufficiently long nanofibrils that they can be considered continuous [Chinga-Carrasco *et al*., 2011]. Conversely, wood fibers have typical lengths between 1 and 3 mm and typical widths between roughly 10 and 50 µm (Figure 17b). The higher aspect ratio (i.e. the length to diameter ratio) of MFC fibrils compared to wood fibers eventually results in an enhanced ability to interact with other molecules, such as lysozyme, being higher the number of binding sites available per unit volume.

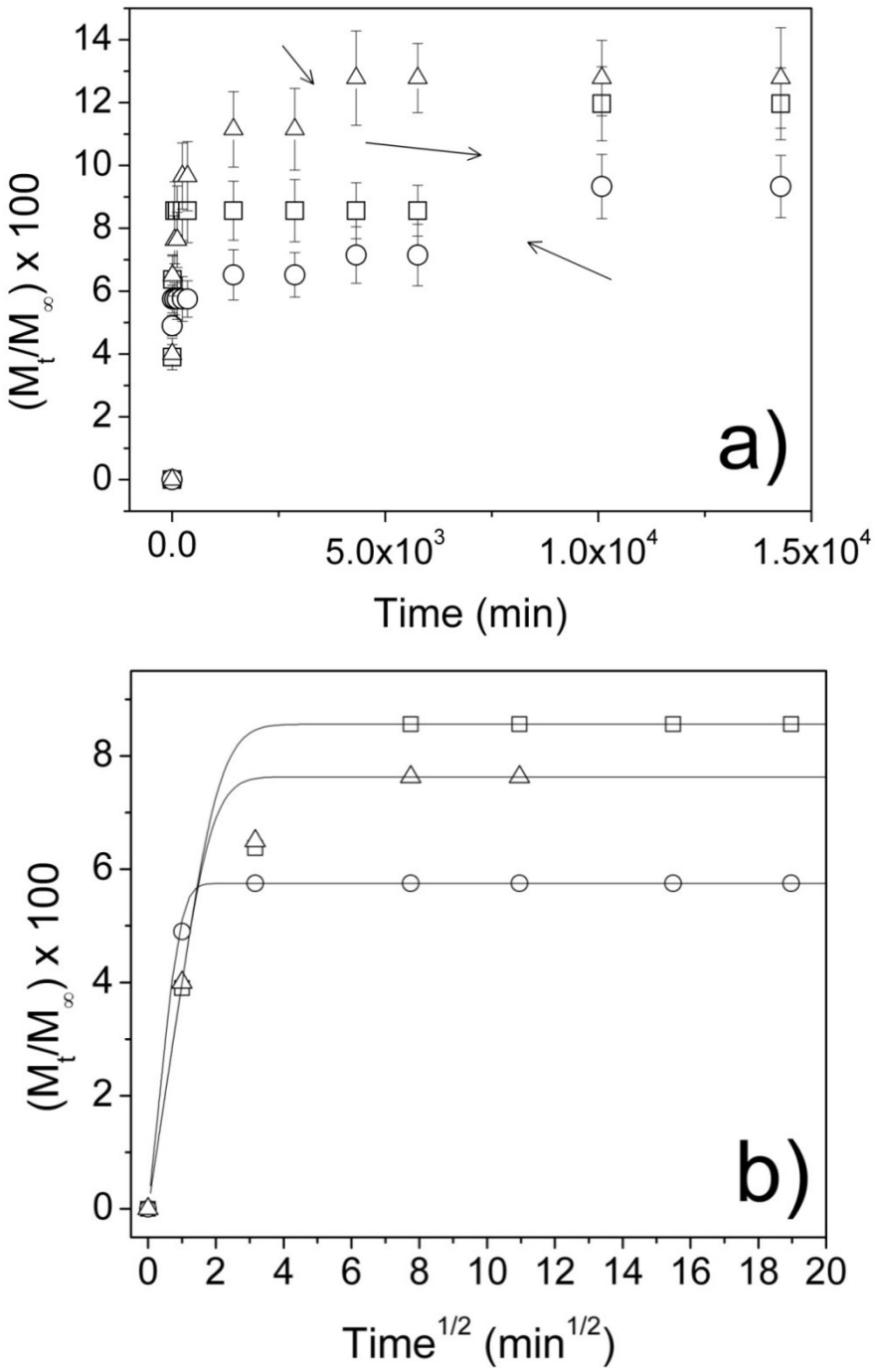

Figure 12. Experimental (a) and calculated (b) release data of lysozyme from samples M-L10 (—□—), M-L10-G4, (—○—), and M-L10-N10 (—△—) after 10 days (a) and 6 hours (b) immersion at 6°C in simulant A.

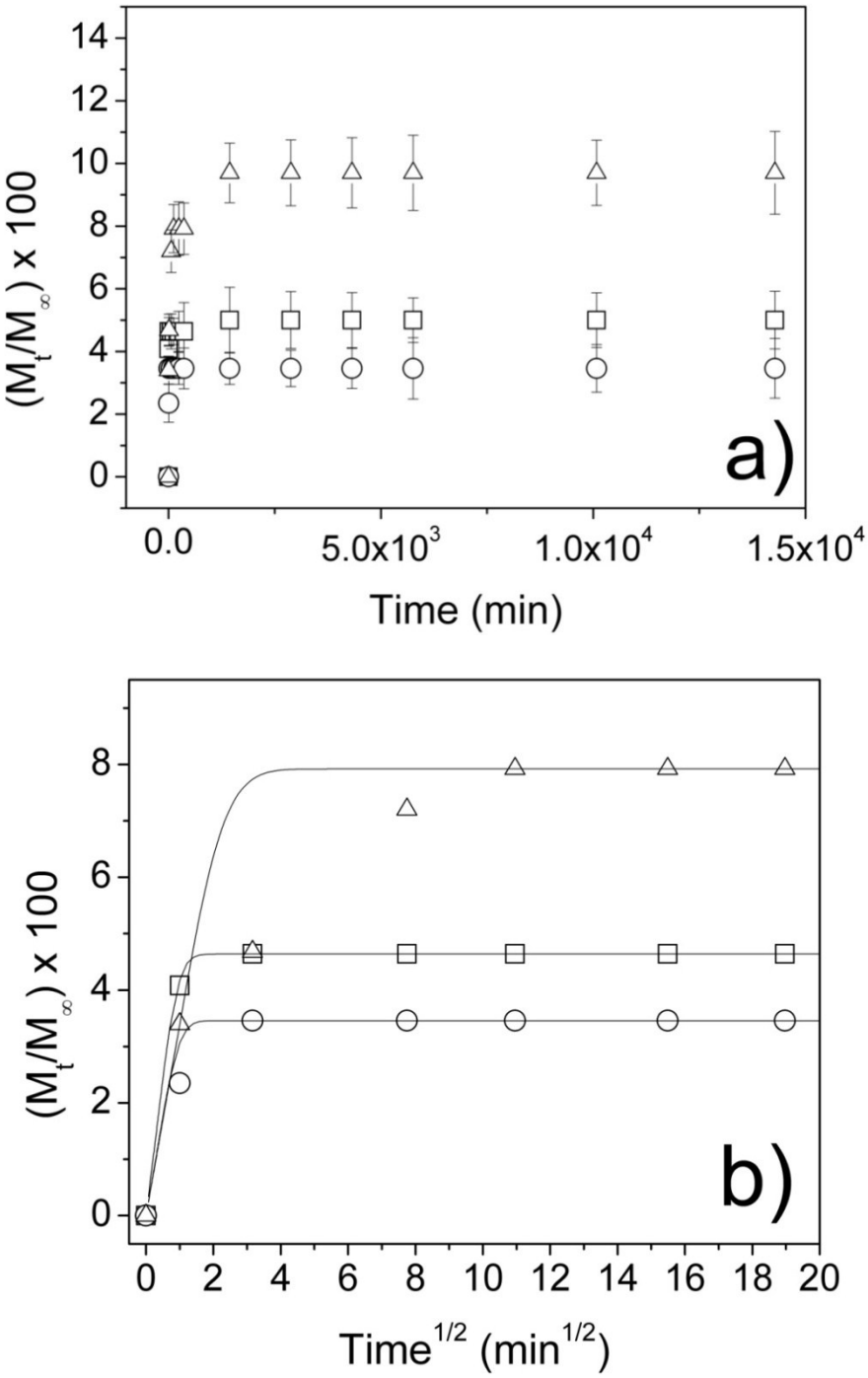

Figure 13. Experimental (a) and calculated (b) release data of lysozyme from samples M-L10 (—□—), M-L10-G4, (—○—), and M-L10-N10 (—△—) after 10 days (a) and 6 hours (b) immersion at 6°C in simulant C.

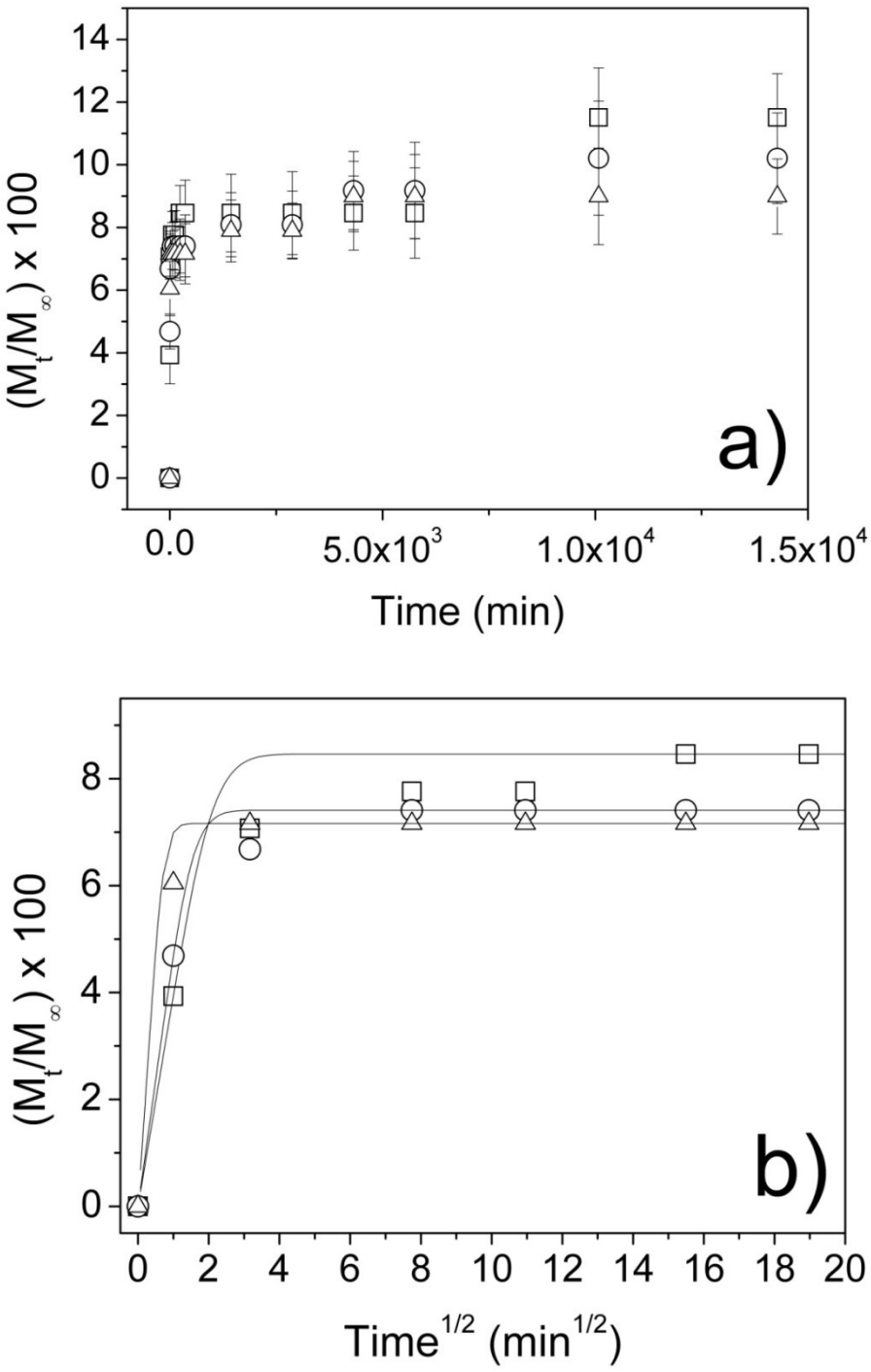

Figure 14. Experimental (a) and calculated (b) release data of lysozyme from samples M-L10 (—□—), M-L10-G4, (—○—), and M-L10-N10 (—△—) after 10 days (a) and 6 hours (b) immersion at 23°C in simulant A.

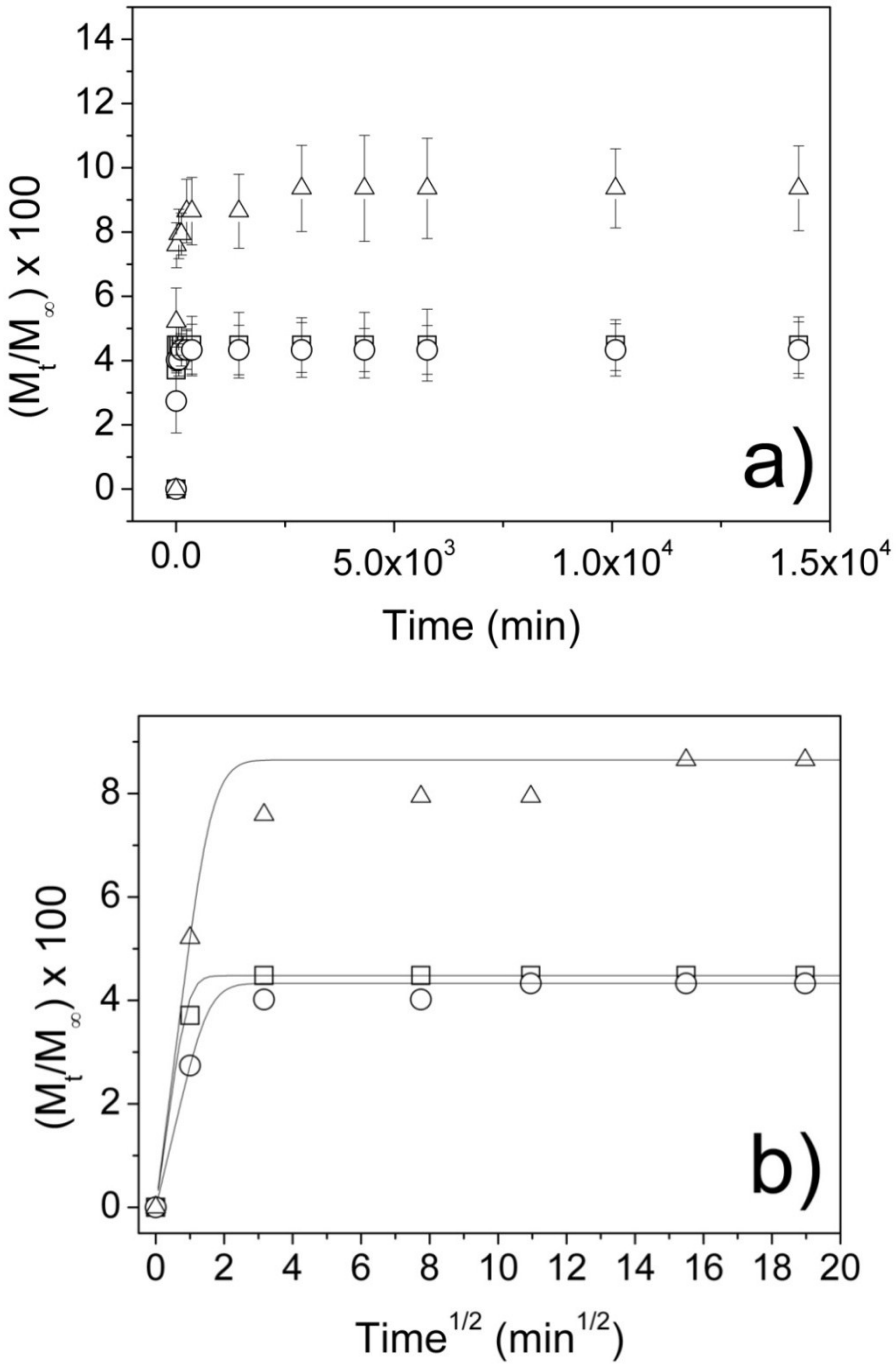

Figure 15. Experimental (a) and calculated (b) release data of lysozyme from samples M-L10 (—□—), M-L10-G4, (—○—), and M-L10-N10 (—△—) after 10 days (a) and 6 hours (b) immersion at 23°C in simulant C.

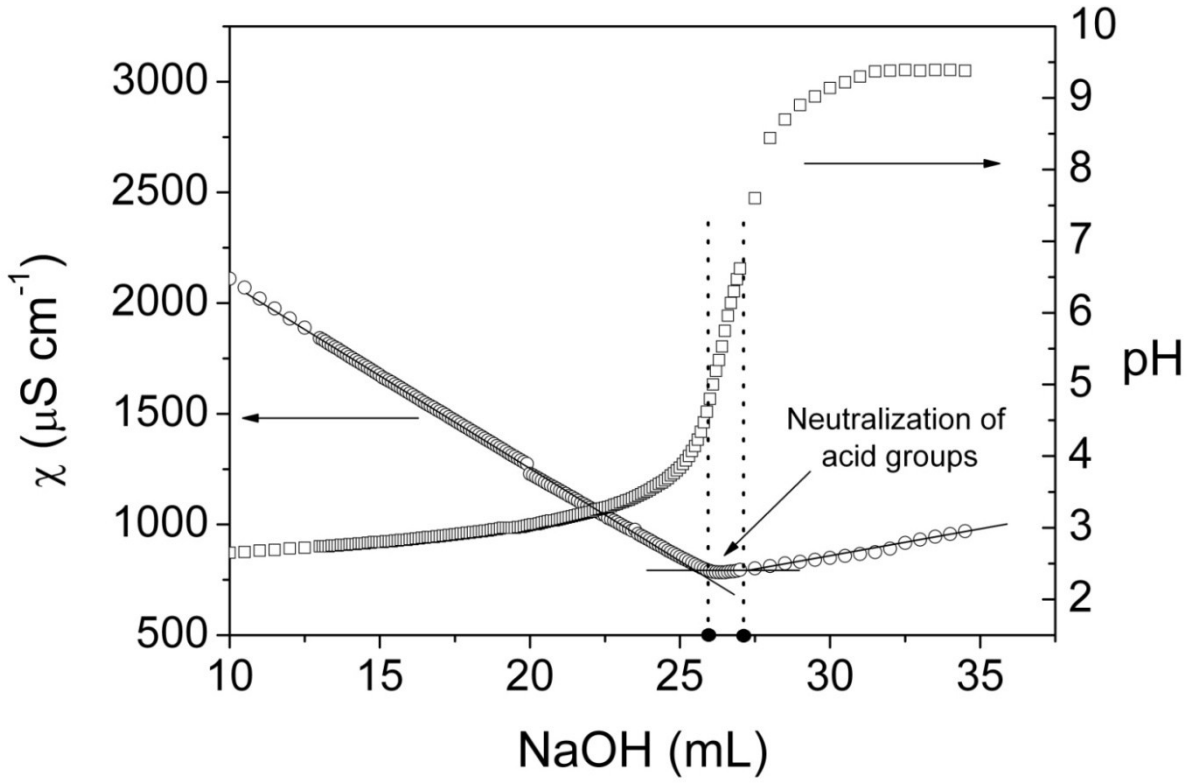

Figure 16. Mean conductometric and potentiometric titration curves for MFC.

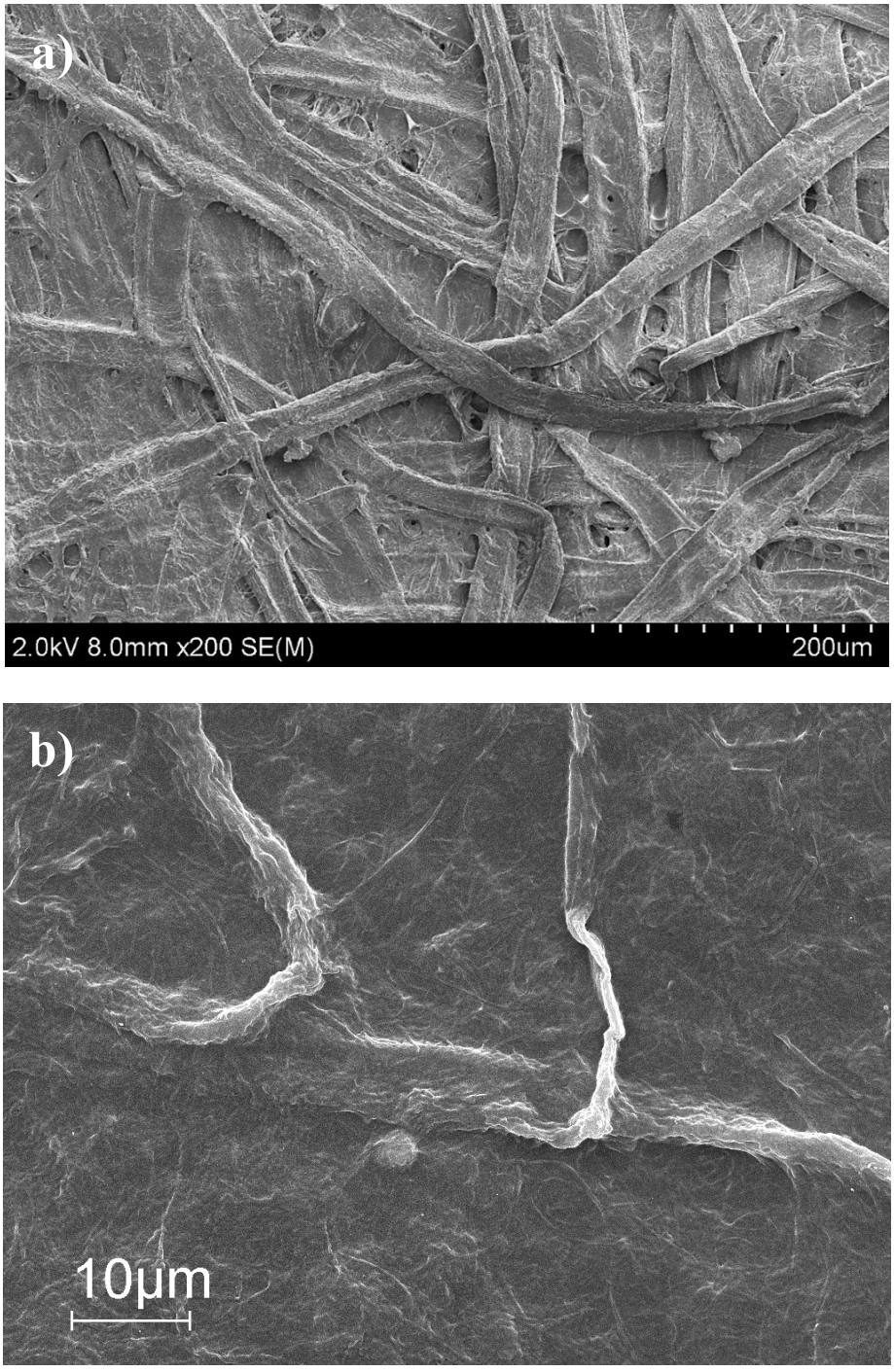

Figure 17. SEM images of raw cellulosic fibers (a) and MFC fibrils (b).

4.2.2 Influence of the type of simulant

It is also interesting to note that, for a same polymer system under the same temperature condition, the total amount of lysozyme released was always higher for the simulant A compared with the simulant C. This probably reflects the hydrophilic nature of the antimicrobial molecule, namely its higher affinity towards water rather than ethanol. At the same time, while water is a strong solvent for the polymer matrix, ethanol has only partial affinity with MFC, thus triggering the release of the active compound to a less extent. However, this observation (higher release values for the simulant A) is not supported by the estimation of the apparent diffusion coefficients, as shown in Table 5. This can be tentatively explained considering that the overall release kinetics obtained from the hydro-alcoholic solution are exclusively governed by the diffusion process of the active molecule across the polymer network to the medium; conversely, when only water was used as a simulant, it can be clearly seen that, while the diffusion process is predominant in the first rising part of each curve, after a certain time secondary effects came about, as indicated by the sudden jumps observable in the lysozyme release evolution (see arrows in Figure 12a). As already reported [Cozzolino *et al.*, 2012], the appearance of the film burst in hydrophilic polymers can be reasonably attributed to the partial collapse of semi-crystalline regions, which certainly occurs after the dissolution of the amorphous phase. The final result was an increase in the total amount of lysozyme released into the surrounding medium (water).

Film type	*l* (μm)	*D* (cm^2/s)				*Sq* (μm)
		6°C		23°C		
		Simulant A	Simulant C	Simulant A	Simulant C	
M-L10	$21.67^{a} \pm 1.15$	$2.2E\text{-}11^{c}$	$1.2E\text{-}10^{d}$	$2.1E\text{-}11^{c}$	$1.3E\text{-}10^{d}$	$0.867^{h} \pm 0.040$
M-L10-G4	$22.33^{a} \pm 0.58$	$1.0E\text{-}10^{d}$	$1.0E\text{-}10^{d}$	$4.0E\text{-}11^{g}$	$4.0E\text{-}11^{g}$	$0.815^{i} \pm 0.031$
M-L10-N10	$16.67^{b} \pm 0.68$	$1.5E\text{-}11^{e}$	$1.0E\text{-}11^{f}$	$1.2E\text{-}10^{d}$	$2.0E\text{-}11^{c}$	$0.885^{h} \pm 0.024$

Different superscripts within a group (i.e. within each parameter) denote a statistically significant difference ($p < 0.05$).

Table 5. Thickness (*l*), diffusion coefficient (*D*), and surface roughness (*Sq*) of the MFC-based films.

4.2.3 Influence of temperature

As far as the influence of the temperature on the release patterns is concerned, there was not statistical difference between samples stored at 6°C and 23°C, which led to the conclusion that the increase in temperature cannot be considered a trigger in the release of lysozyme from the MFC-based films, at least within the experimental thermal range tested in this work. Most likely this is due to the low sensitivity of MFC to changes in temperature. Indeed, as most cellulosic materials, the thermal properties of MFC, intimately linked to its highly cohesive nature (with a glass transition temperature higher than its degradation temperature) mainly driven by extensive hydrogen bonding, allows the polymer matrix to preserve almost entirely its physical arrangement even after the temperature shift 6°C → 23°C [Lavoine *et al*., 2012; Moon *et al*., 2011]. This finding can have a relevant importance from a practical point of view: the release of lysozyme would not be affected by different storage conditions (i.e., temperature) of the MFC-based package.

4.2.4 Influence of glycerol and NaCl

Finally, the effect due to the use of the two modulating agents is discussed. As it can be gathered from the values of the apparent diffusion coefficients for the samples M-L10 and M-L10-G4 (Table 5), glycerol, as expected, triggered the release of the active molecule in the water medium (simulant A) at both temperatures (6°C and 23°C), due to its well-known plasticizing effect [Trovatti *et al*., 2012]. However, the loaded amount of glycerol (4 wt.%) probably was not enough to impart such changes in the MFC physical structure (i.e., increase in the free volume) to rise significantly the total amount of lysozyme released. In addition, new established interactions between glycerol molecules and the main polysaccharide backbone have also been suggested [Trovatti *et al*., 2012]. Eventually, this competition between glycerol and lysozyme to bind the main MFC chains would have led to an increase in the amount of antimicrobial molecule released to the water medium. Conversely, glycerol thwarted the release of lysozyme from the MFC matrix when exposed to the hydro-alcoholic medium (simulant C). As already reported in a similar study, it is plausible that water-ethanol-glycerol interactions modify the availability of water molecules toward the polymer matrix, thus slowing down the relaxation of the polymer chains [Cozzolino *et al*., 2012]. As far as the effect of the NaCl is concerned, the addition of the salt apparently hindered the release of lysozyme. This can be attributed to changes in the MFC molecular arrangement driven by the

presence of the salt. More specifically, while in low-concentration regime fibril-fibril interactions are prevented by the electrostatic repulsion between negatively charged groups, aggregation is prompted as the ionic strength is increased (screening effect) [Fall *et al*., 2011]. This was demonstrated by the thickness measured for the different MFC films. As shown in Table 5, the difference in thickness between the NaCl-loaded samples (M-L10-N10) and the other two samples (M-L10 and M-L10-G4) was statistically significant, being the sample M-L10-N10 'shrunk' (i.e., lower thickness) owing to the salt-induced fibrils aggregation.

4.2.5 Surface morphology of the MFC-based films

The final morphology of a film (both of plastic and natural origin) is an important parameter especially as it may dramatically affect interfacial phenomena such as wettability, light scattering, ease of contamination [Farris *et al*., 2011; Introzzi *et al*., 2012]. In turn, this would be reflected in some final properties of the films (e.g., optical properties), but also in several finishing operations such as deposition of protective coatings, printing, lamination, to which the films can be subjected after fabrication. An overall view of the surface topography of the three MFC-based samples is provided in Figure 18. As reported in Table 5, although there was not a big difference among samples, the glycerol-loaded one (M-L10-G4) exhibited the smoothest surface, while there was not a statistically significant difference between the films M-L10 and M-L10-N10. It may plausible that the addition of glycerol reduced the intra-/intra-molecular aggregation of cellulose fibrils, leading to an overall relaxation of the MFC network, hence to a less 'bumpy' surface. On the contrary, the highest surface roughness measured for the M-L10-N10 films corroborated the aforementioned salt-induced aggregation of MFC fibrils.

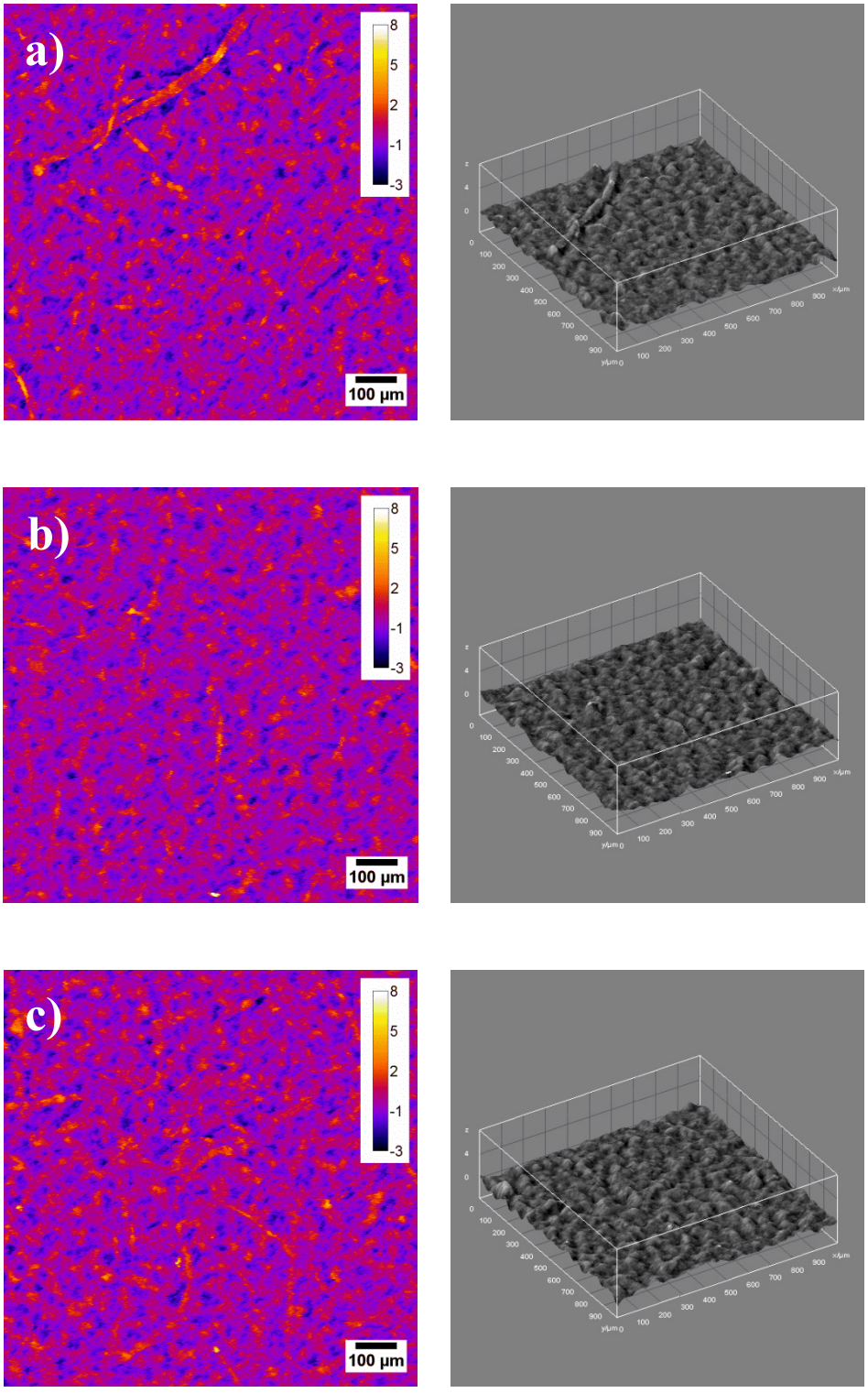

Figure 18. Laser profilometry (left) and 3D (right) images of samples M-L10 (a), M-L10-G4 (b) and M-L10-N10 (c).

5 CONCLUSIONS

In the first work - "Dye release behavior from polyvinyl alcohol films in a hydro-alcoholic medium: influence of physicochemical heterogeneity" - the different release kinetics of a small molecule (Coomassie blue dye) from three different PVOH films into a hydroalcoholic solution were investigated over an extended temporal window (one month). Our results showed that the release from PVOH is mainly controlled by its chemical composition, i.e. the degree of substitution of the acetate groups by hydroxyl groups, which in turn dictates the degree of crystallinity, as unequivocally demonstrated by diffraction, thermal, and morphological analyses. The crystallinity played an important role in controlling the release properties of the PVOH matrices insomuch as the final release system can be reasonably considered as a crystal dissolution-controlled system. Molecular weight was shown to affect the overall release properties to a less extent. Apparently, higher level of molecular chain entanglement hindered the mobility of the entrapped molecule through the molecular polymer chains. The use of ethanol also influenced the ultimate release properties of the three PVOH samples. Due to its non-solvent feature toward this polymer, ethanol made possible avoiding both abrupt volumetric expansion and complete dissolution of the matrices over the entire time of analysis. Finally, the affinity between the polymer matrix and the loaded molecule could have promoted the establishment of new weak intermolecular forces, e.g. ion-dipole interactions, which would have somehow affected the final amount of the dye released. These results, together with the mathematical modeling of the release kinetics, can be profitably used for the development of delivery systems for different applications, where the controlled release over time of an active molecule is the target.

In the second work - "Exploiting the nano-sized features of microfibrillated cellulose (MFC) for the development of controlled release packaging" - the still open issue of the controlled release packaging systems was faced under a nanotechnology perspective. Our goal was to demonstrate that the release of a small molecule active compound can be somehow slowed down by exploiting the nano-sized characteristics of the polymer network. Indeed, the microfibrillated cellulose films used in this work were successfully demonstrated to be a suitable carrier for the antimicrobial lysozyme, preventing its fast release during the early stages of contact with the two food stimulants tested (water and water/ethanol solutions). However the observed performance, which was attributed to an 'interface effect', yielded

over-retention of the active molecule in the final films. The MFC release systems were also insensitive to changes in temperature (6°C and 23°C), a feature that can profitably used for practical applications (e.g., packaged food). The use of two modulating agent also showed that the release can be to some extent fine-tuned acting on the physicochemical properties (e.g., the aggregation state of the fibrils) of the main MFC network.

Finally, one of the problems of the use of nanotechnology in food packaging will certainly be the way consumers generally very reluctant to accept new technologies in food than in other consumer products. This obstacle can be overcome only if governments and industries will be able to instill consumer confidence by protecting them from the potential risks (mostly still in the evaluation phase) of the use and abuse of nanomaterials. These include the nanomaterial migration through polymer films, the interaction of nanomaterial biomolecules and cellular components, the interrelationships between nanoparticle characteristics, their toxicity and pharmacokinetic properties, in addition to the biodegradability of nanomaterials. As with any new technology, there should be a continuous dialogue between the scientists, companies and consumers, bearing in mind the potential risks and ethical problems that may arise. If we succeed in this endeavor, the advantages of nanotechnology can play an important role in making the world's food supply healthier, safer and more plentiful. Last but not least, is the economic impact that nanotechnology will have: $ 3 trillion by 2020, with a requirement of at least 6 million workers to support them by the end of the decade (Duncan, 2011).

6 OTHER WORKS

6.1 PAPER III

'Wetting enhancer' pullulan coating for anti-fog packaging applications.

Introzzi L., Fuentes-Alventosa J.M., Cozzolino C.A., Trabattoni S., Tavazzi S., Schiraldi A., Piergiovanni L., Farris S. **Applied Materials & Interfaces**, 2012, 4: 3692−3700.

In this work is described a new antifog coating made of pullulan. The antifog properties are discussed in terms of wettability, surface chemistry/morphology and by quantitative assessment of the optical properties (haze and transparency), before and after fog formation. The work also presents the results of antifog tests simulating the typical storage conditions of fresh foods. In these tests, the antifog efficiency of the pullulan coating was compared with that of two commercial antifog films, whereas an untreated low density polyethylene (LDPE) film was used as a reference. The obtained results revealed that the pullulan coating behaved as a "wetting enhancer", mainly due to the low water contact angle (~24°), which in turn can be ascribed to the inherent hydrophilic nature of this polysaccharide, as also suggested by the X-ray photoelectron spectroscopy experiments. Unlike the case of untreated LDPE and commercial antifog samples, no discrete water formations (i.e., droplets or stains) were observed on the antifog pullulan coating on refrigeration during testing. Rather, an invisible, continuous and thin layer of water occurred on the biopolymer surface, which was the reason for the unaltered haze and increased transparency, with the layer of water possibly behaving as an antireflection layer. As confirmed by atomic force microscopy analysis, the even deposition of the coating on the plastic substrate compared to the patchy surfacing of the antifog additives in the commercial films is another important factor dictating the best performance of the antifog pullulan coating.

6.2 PAPER IV

A green nanocomposite: Pullulan Films Reinforced with MFC.

Cozzolino C.A., Piga A., Farris S. **Manuscript**, 2012 (in preparation).

The goal of this study was the development a green nanocomposite obtained from pullulan and MFC, a cellulose-derived nanomaterial. The incorporation of MFC led to an increase in:

i) mechanical properties, such as bending/tensile strength and Young's modulus; ii) thermal stability and iii) barrier properties. This is still an ongoing work within our labs in Milan.

6.3 PAPER V

Qualità e sicurezza dei prodotti vegetali minimamente trattati (IV gamma) attraverso imballaggi plastici funzionali. **Quaderni della Ricerca**, 2012, vol. 143. Regione Lombardia Agricoltura. [VEGAPACK PROJECT]

Approved in 2009, Vegapack Project concerned to optimize the quality and safety of minimally processed vegetable products through functional plastic packages, using a soluble compound (LAE) and a volatile compound (carvacrol). In this project, I studied the incorporation of LAE in biopolymer coatings (i.e. gelatin based). LAE is a derivative of lauric acid, *L*-arginine and ethanol, with positive charge. The main characteristics of this molecule are a wide range of antimicrobial properties derived from its surfactant chemical structure that additionally yields certain tensioactive properties. LAE proved Generally Regarded As Safe (GRAS) and its use in food field was authorized by FDA in 2005 and as food additive by EFSA (European Food Safety Autority) in 2007.

7 ACKNOWLEDGEMENTS

First, I would like to express my gratitude to my supervisor Prof. Antonio Piga, Prof. Antonio Farris and Prof. Budroni for giving me the opportunity to do this work and for believing in me; besides all my collegues of STAA, Department of Agriculture, University of Sassari.

Most of my research studies were made by DeFENS, Department of Food, Environmental and Nutritional Sciences, Packaging Division, University of Milan. About this, I must thank my tutor, Prof. Luciano Piergiovanni, for having welcome in the Packlab big family. Guys, with you I spent three years of research, discussions, problem sharing and moments of lab painting... thanks for everything!

During this experience I was so lucky to spend part of my reaserch in Norway by Paper and Fiber Research Institute (PFI) and by Norwegian University of Science and Technology (NTNU). I want to thank docs. Marco Iotti, Philip André Reme, Gary Chinga-Carrasco, Sara Paunonen, Prof. Størker Moe, and all the other collegues for having hosted me in their group, listened to me and always given me advices. Vennlig hilsen!
A very special thank to my roommates Luis (Brazil), Ludmilla (Argentina), Clémence (France) and Laura (Spain). It was a pleasure sharing apartment and experiences with you. Thank you very much!

Last, but not least, thanks to Stefano, my scientific mentore and friend, for scientific discussions, chats, advices and encouragement. This thesis is also a bit yours.

To Silvia. Because you were always there for me and there aren't words. You know.

8 REFERENCES

Abe K., Iwamoto S., Yano H. *Biomacromolecules* **2007**, 8, 3276-3278.

Ahola S., Salmi J., Johansson L.S., Laine J., Österberg M. *Biomacromolecules* **2008**, 9, 1273-1282.

Alen R., in Stenius P. (Ed.), Forest products chemistry, Papermaking Science and Technology, Vol. 3, FapetOy, Helsinki, Finland, **2000**, 58–104.

Andresen M. and Stenius P. *J. Dispers. Sci. Technol.* **2007**, 28(6), 837-844.

Andresen M., Stenstad P., Møretrø T., Langsrud S., Syverud K., Johansson L.S., Stenius P. *Biomacromolecules* **2007**, 8(7), 2149-2155.

Asran A.S., Henning S., Michler G.H. *Polymer* **2010**, 51, 868‑876.

Assender H.E. and Windle A.H. *Polymer* **1998**, 39, 4295-4302.

Aulin C., Varga I., Claesson P.M., Wågberg L., Lindström T. *Langmuir* **2008**, 24, 2509-2518.

Balasubramanian A., Lee D.S., Chikindas M., Yam K. *Probiotics Antimicrob. Proteins* **2011**, 3(2), 113-118.

Berglund L., New concepts in natural fibres composites, 27th Risø international symposium on material science, Risø National Laboratory, Roskilde, Denmark, **2006**.

Boroglu M.S., Celik S.U., Bozkurt A., Boz I. *J. Membr. Sci.* **2011**, 375, 157‑164.

Bunn C.W. *Nature* **1948**, 161, 929-930.

Buonocore G.G., Del Nobile M.A., Panizza A., Corbo M.R., Nicolais L. *J. Control. Release* **2003**, 90, 97-107.

Burger C., Hsiao B.S., Chu B. *Annu. Rev. Mater. Res.* **2006**, 36, 333-368.

Cabiaca A., Guillon E., Chambon F., Pinel C., Rataboul F., Essayem N. *Appl. Catal. A-Gen.* **2011**, 402, 1-10.

Canfield R.E. and Liu A.K. *J. Biol. Chem.* **1965**, 240, 1997-2002.

Chial H.J., Thompson H.B., Splittgerber A.G. *Anal. Biochem.* **1993**, 209, 258-266.

Chiellini E., Cinelli P., Ilieva V.I., Martera M. *Biomacromolecules* **2008**, 9, 1007‑1013.

Chinga-Carrasco G. *Nanoscale Res. Lett.* **2011**, 6, 417.

Chinga-Carrasco G., Miettinen A., Luengo Hendriks C.L., Gamstedt E.K., Kataja M. Structural Characterisation of Kraft Pulp Fibres and Their Nanofibrillated Materials for Biodegradable Composite Applications. *In*: Nanocomposites and Polymers with Analytical Methods - Book 3, ISBN 979-953-307-136-6., **2011**, 243-260.

Commission Regulation (EU) No 10/2011of 14 January **2011** on plastic materials and articles intended to come into contact with food, Official Journal of the European Union, L 12/1 L 12/89.

Costa D., Valente A.J.M., Miguel M.G., Lindman B. *Colloid Surf. A* **2011**, 391, 80‑87.

Cozzolino C.A., Blomfeldt T.O.J., Nilsson F., Piga A., Piergiovanni L., Farris S. *Colloid. Surface. A* **2012**, 403, 45-53.

Crank J. The Mathematics of Diffusion, Clarendon Press, Oxford, **1975**.

Dainelli D., Gontard N., Spyropoulos D., Zondervan-van den Beukend E., Tobback P. *Trends Food Sci. Technol.* **2008**, 19, 103‑112.

De Prisco N., Immirzi B., Malinconico M., Mormile P., Petti L., Gatta G. *J. Appl. Polym. Sci.* **2002**, 86, 622‑632.

Dicharry R.M., Ye P., Saha G., Waxman E., Asandei A.D., Parnas R.S. *Biomacromolecules* **2006**, 7, 2837‑2844.

Doppers L.M., Breen C., Sammon C. *Vib. Spectrosc.* **2004**, 35, 27-32.

Duncan T.V. *J. Colloid. Interf. Sci.* **2011**, 363, 1‑24.

Fall A.B., Lindström S.B., Sundman O., Ödberg L., Wågberg L. *Langmuir* **2011**, 27, 11332-11338.

Farris S., Introzzi L., Biagioni P., Holz T., Schiraldi A., Piergiovanni L. *Langmuir* **2011**, 27, 7563-7574.

Farris S., Mora L., Capretti G., Piergiovanni L. *J. Chem. Educ.* **2012**, 89, 121-124.

Farris S., Schaich K.M., Liu L.S., Piergiovanni L., Yam K.L. *Trends Food Sci. Tech.* **2009**, 20, 316-332.

Faruk O, Bledzki A.K., Fink H.P., Sain M. *Prog. Polym. Sci.* **2012**, 37, 1552-1596.

Finch C.A. Poly(vinyl alcohol): properties and applications, John Wiley and Sons, New York, **1973**.

Fox T.G. and Flory P.J. *J. Appl. Phys.* **1950**, 21, 581-591.

Freudenberg U., Zimmermann R., Schmidt K., Behrens S.H., Werner C. *J. Colloid. Interf. Sci.* **2007**, 309, 360-365.

Fuchs O. Polymer Handbook, third ed., John Wiley and Sons, New York, **1989**.

Gedde U.W. Polymer Physics, Kluwer Academic Publishers, Dordrecht, **1995**.

Gemili S., Yemenicioğlu A., Altınkay S.A. *J. Food Eng.* **2009**, 90, 453-462.

Gemili S., Yemenicioglu A., Altınkaya S.A. *J. Food Eng.* **2010**, 96, 325-332.

Hassan C.M. and Peppas N.A.A. *Adv. Polym. Sci.* **2000**, 153, 37-65.

Herrick F.W., Casebier R.L., Hamilton J.K., Sandberg K.R. *J. Appl. Polym. Sci.: Appl. Polym. Symp.* **1983**, 37, 797-813.

Hodge R.M., Bastow T.J., Edward G.H., Simon G.P., Hill A.J. *Macromolecules* **1996 (II)**, 29, 8137-8143.

Hodge R.M., Edward G.H., Simon G.P. *Polymer* **1996 (I)**, 37, 1371-1376.

Huang J., Kao H., Wu X.Y. *J. Control. Release* **2000**, 67, 45‑54.

Hubbe M.A., Rojas O.J., Lucia L.A., Sain M. *Bio Res.* **2008**, 3(3), 929-980.

Hult E.L., Iotti M., Lenes M. *Cellulose* **2010**, 17, 575-586.

Ibrahim H.R., Higashiguchi S., Koketsu M., Juneja L.R., Kim M., Yamamoto T., Sugimoto Y., Aoki T. *J. Agric. Food Chem.* **1996**, 44, 3799-3806.

Introzzi L., Fuentes-Alventosa J.M., Cozzolino C.A., Trabattoni S., Tavazzi S., Bianchi C.L., Schiraldi A., Piergiovanni L., Farris S. *ACS Appl. Mater. Interfaces* **2012**, 4, 3692-3700.

Iotti M., Gregersen Ø.W., Moe S., Lenes M. *J. Polym. Environ.* **2011**, 19, 137-145.

Iwamoto S., Nakagaito A.N., Yano H. *Appl. Phys. A* **2007**, 89, 461-466.

Jin X. and Hsieh Y.L. *Polymer* **2005**, 46, 5149‑5160.

Joerger R.D. *Packag. Technol. Sci.***2007**, 20, 231-273.

Juntanon K., Niamlang S., Rujiravanit R., Sirivat A. *Int. J. Pharm.* **2008**, 356, 1‑11.

Kaplan D.L., Mayer J.M., Ball D., McCassie J., Stenhouse S. Fundamentals of biodegradable polymers, in: Ching C., Kaplan D.L., Thomas E.L. (Eds.), Biodegradable Polymers and Packaging, Technomic Publishing Inc., Lancaster, **1993**, p. 152.

Kim G.M., Asran A.S., Michler G.H., Simon P., Kim J.S. *Bioinspir. Biomim.* **2008**, 3, 1-12.

Klee S.K., Farwick M., Lersch P. *Colloid. Surf. A* **2009**, 338, 162‑166.

Klemm D., Kramer F., Moritz S., Lindström T., Ankerfors M., Gray D., Dorris A. *Angew. Chem. Int. Ed.* **2011**, 50, 5438-5466.

Klemm D., Schumann D., Kramer F., Heßler N., Hornung M., Schmauder H.P., Marsch S. *Adv. Polym. Sci.* **2006**, 205, 49-96.

Kobayashi M., Toguchida J., Oka M. *Biomaterials* **2003**, 24, 639‑647.

Labuschagne P.W., Germishuizen W.A., Verryn S.M.C., Moolman F.S. *Eur. Polym. J.* **2008**, 44, 2146‑2152.

LaCoste A., Schaich K.M., Zumbrunnen D., Yam K.L. *Packag. Technol. Sci.* **2005**, 18, 77-87.

Langer R. and Peppas N. *Macromol. Chem. Phys.* **1983**, C23, 61-126.

Lavoine N., Desloges I., Dufresne A., Bras J. *Carbohyd. Polym.* **2012**, 90, 735-764.

Li B., Kennedy J.F., Peng J.L., Yie X., Xie B.J. *Carbohyd. Polym.* **2006**, 65, 488-494.

Li J.K., Wang N., Wu X.S. *J. Control. Release* **1998**, 56, 117‑126.

Liang S., Huang Q., Liu L., Yam K.L. *Macromol. Chem. Phys.* **2009**, 210, 832‑839.

Liu H.B., Yan Q., Wang C., Liu X., Wang C., Zhou X.H., Xiao S.J. *Colloid Surf. A* **2011**, 386, 131‑134.

López-Rubio A., Lagaron J.M., Ankerfors M., Lindström T., Nordqvist D., Mattozzi A., Hedenqvist M.S. *Carbohydr. Polym.* **2007**, 68, 718-727.

Lu J., Wang T., Drzal L.T. *Compos. Part A-Appl. S.* **2008**, 39, 738-746.

Mallapragada S.K. and Peppas N.A. *J. Control. Release* **1997**, 45, 87‑94.

Marino I.G., Lottici P.P., Razzetti C., Montenero A., Rocchetti M., Toselli M., Marini M., Pilati F. *Packag. Technol. Sci.* **2008**, 21, 329‑338.

Martien F.L. Encyclopedia of Polymer Science and Engineering, John Wiley and Sons, New York, **1986**.

Martins N.C.T., Freire C.S.R., Pinto R.J.B., Fernandes S.C.M., Neto C.P., Silvestre A.J.D., Causio J., Baldi G., Sadocco P., Trindade T. *Cellulose* **2012**, 19(4), 1425-1436.

Mascheroni E., Capretti G., Marengo M., Iametti S., Mora L., Piergiovanni L., Bonomi F. *Packag. Technol. Sci.* **2010**, 23, 47-57.

Mastromatteo M., Barbuzzi G., Conte A., Del Nobile M.A. *Innov. Food Sci. Emerg.* **2009**, 10, 222-227.

Moon R.J., Martini A., Nairn J., Simonsen J., Youngblood J. *Chem. Soc. Rev.* **2011**, 40, 3941-3994.

Moreno I., Gonzalez-Gonzalez V., Romero-Garcia J. *Eur. Polym. J.* **2011**, 47, 1264‑1272.

Moreno M., Hernandez R., Lopez D. *Eur. Polym. J.* **2010**, 46, 2099‑2104.

Morita R., Honda R., Takahashi Y. *J. Control. Release* **2000**, 63, 297-304.

Nirmala R., Kalpana D., Jeong J.W., Oh H.J., Lee J.H., Navamathavan R., Lee Y.S., Kim H.Y. *Colloid Surf. A* **2011**, 384, 605‑611.

Onofre F., Wang Y.J., Mauromoustakos A. *Carbohyd. Polym.* **2009**, 76, 541-547.

Pääkkö M., Vapaavuori J., Silvennoinen R., Kosonen H., Ankerfors M., Lindström T., Berglund L.A., Ikkala O. *Soft Matter* **2008**, 4, 2492-2499.

Park J.S., Park J.W., Ruckenstein E. *Polymer* **2001**, 42, 4271‑4280.

Peppas N. and Merrill E. *J. Appl. Polym. Sci.* **1976**, 20, 1457-1465.

Poursamar S.A., Azami M., Mozafari M. *Colloid Surf. B* **2011**, 84, 310‑316.

Quintavalla S. and Vicini L. *Meat Sci.* **2002**, 62, 373-380.

Restuccia D., Spizzirri U.G., Parisi O.I., Cirillo G., Curcio M., Iemma F., Puoci F., Vinci G., Picci N. *Food Control* **2010**, 21, 1425-1435.

Rodríguez A., Batlle R., Nerín C. *Prog. Org. Coat.* **2007**, 60, 33-38.

Sakurada I., Nukushina Y., Sone Y. *Kobunshi Kagaku* **1955**, 12, 510-513.

Schwenter F., Bouche N., Pralong W.F., Aebischer P. *Biomaterials* **2004**, 25, 3861‑3868.

Shaheen S.M. and Yamaura K. *J. Control. Release* **2002**, 81, 367‑377.

Simão P. Pinho and Eugénia A. Macedo *J Chem Eng Data* **2005**, 50, 29-32.

Siqueira G., Bras J., Dufresne A. *Polymers* **2010**, 2, 728-765.

Siró I. and Plackett D. *Cellulose* **2010**, 17, 459-494.

Small E.F., Willy M.C., Lewin P.A., Wrenn S.P. *Colloid Surf. A* **2011**, 390, 40‑47.

Srithep Y., Turng L.S., Sabo R., Clemons C. *Cellulose* **2012**, 19(4), 1209-1223.

Sudhamani S.R., Prasad M.S., Sankar K.U. *Food Hydrocolloids* **2003**, 17, 245‑250.

Sung J.H., Hwang M.R., Kim J.O., Lee J.H., Kim Y.I., Kim J.H., Chang S.W., Jin S.G., Kim J.A., Won Lyoo W.S., Han S.S., Ku S.K., Yong C.S., Choi H.G. *Int. J. Pharm.* **2010**, 392, 232‑240.

Syverud K. and Stenius P. *Cellulose* **2009**, 16, 75-85.

Syveruda K., Chinga-Carrasco G., Toledo J., Toledo P.G. *Carbohydr. Polym.* **2011**, 84, 1033-1038.

Tanigami T., Yano K., Yamaura K., Matsuzawa S. *Polymer* **1995**, 36, 2941-2946.

Thomas N.L. and Windle A.H. *Polymer* **1980**, 21, 613-619.

Trovatti E., Fernandes S.C.M., Rubatat L., da Silva Perez D., Freire C.S.R., Silvestre A.J.D., Neto C.P. *Compos. Sci. Technol.* **2012**, 72, 1556-1561.

Tunç S. and Duman O. *Food Sci. Technol.-Leb.* **2011**, 44, 465-472.

Turbak A.F., Snyder F.W., Sandberg K.R. *J. Appl. Polym. Sci.: Appl. Polym. Symp.* **1983**, 37, 815-827.

Virtanen T., Maunu S.L., Tamminen T., Hortling B., Liitiä T. *Carbohyd. Polym.* **2008**, 73, 156-163.

Wu S., Li F., Wang H., Fu L., Zhang B., Li G. *Polymer* **2010**, 51, 6203‑6211.

Yeh K.W., Chang C.P., Yamamoto T., Dobashi T. *Colloid. Surf. A* **2011**, 380, 152‑155.

Yılmaz G., Ongen G., Jongboom R.O.J., Feil H., van Dijk C., Hennink W.E. *Biomacromolecules* **2002**, 3, 305-311.

Yun J., Im J.S., Lee Y.S., Bae T.S., Lim Y.M., Kim H.I. *Colloid Surf. A* **2010**, 368, 23‑30.

Yun S., Im H., Heo Y., Kim J. *J. Membr. Sci.* **2011**, 380, 208‑215.

Zhang Y., Chikindas M.L., Yam K.L. *Int. J. Food Microbiol.* **2004**, 19 (1), 15-22.

APPENDIX

Paper I

"*Dye release behavior from polyvinyl alcohol films in a hydro-alcoholic medium: influence of physicochemical heterogeneity*"

Cozzolino C.A., Blomfeldt T. O.J., Nilsson F., Piga A., Piergiovanni L., Farris S.

Colloids and Surfaces A: Physicochemical and Engineering Aspects, 2012, 403: 45– 53

Colloids and Surfaces A: Physicochem. Eng. Aspects 403 (2012) 45–53

Contents lists available at SciVerse ScienceDirect

Colloids and Surfaces A: Physicochemical and Engineering Aspects

journal homepage: www.elsevier.com/locate/colsurfa

Dye release behavior from polyvinyl alcohol films in a hydro-alcoholic medium: Influence of physicochemical heterogeneity

Carlo A. Cozzolino[a,c], Thomas O.J. Blomfeldt[b], Fritjof Nilsson[b], Antonio Piga[a], Luciano Piergiovanni[c], Stefano Farris[b,c,*]

[a] STAA, Department of Agriculture, University of Sassari, Viale Italia 39/A, 07100 Sassari, Italy
[b] Department of Fiber and Polymer Technology, KTH Royal Institute of Technology, SE-10044 Stockholm, Sweden
[c] DeSTAM, Department of Food Science and Microbiology, Packaging Division, University of Milan, Via Celoria 2, 20133 Milan, Italy

ARTICLE INFO

Article history:
Received 12 December 2011
Received in revised form 7 March 2012
Accepted 23 March 2012
Available online 1 April 2012

Keywords:
Controlled release
Diffusion
Modeling
Morphology
Polyvinyl alcohol

ABSTRACT

In this paper we investigated the release kinetics of a model drug-like compound (Coomassie brilliant blue) from polyvinyl alcohol (PVOH) films into a hydro-alcoholic solution as a function of the physicochemical properties of the polymer matrix. After 33 days of monitoring, the total amount released ranged from 10% for the high hydrolysis degree/low molecular weight PVOH films to 60% for the low hydrolysis degree/low molecular weight films. Mathematical modeling allowed for an estimation of the two diffusion coefficients (D_1 and D_2) that characterized the release profile of the dye from the films. The degree of hydrolysis dramatically affected both the morphology and the physical structure of the polymer network. A high hydroxyl group content was also associated with the shifting of second order and first order transitions toward higher temperatures, with a concurrent increase in crystallinity. Moreover, the higher the degree of hydrolysis, the higher the affinity of the polymer to the negatively charged molecule dye. Selection of the polymer matrix based on physicochemical criteria may help in achieving different release patterns, thereby representing the first step for the production of polymer systems with modulated release properties.

1. Introduction

Polyvinyl alcohol (PVOH) is an attractive polymer for many different applications. It has been widely used in many fields, such as: environmental, for the production of films for the removal of heavy metal ions in water [1]; pharmaceutical, for the obtainment of wound-dressing systems [2] and biomedical, as a scaffold supporting material for tissue engineering applications [3]. Other applications include agriculture [4], packaging [5], fuel cells [6], and electrochemistry [7]. In addition, PVOH is well suited both to produce electrospun nanofibrous mats [8] and to develop polymer blends in association with many biopolymers [9–13]. The success of PVOH is due to many reasons, first of all because of its unique molecular structure and properties, such as its rubbery or elastic nature and its high degree of swelling in aqueous solutions [14]. Moreover, the hydroxyl pendant group on every second carbon atom on its backbone allows PVOH to take part in many chemical cross-linking reactions [15], interact with many other polymers, primarily through hydrogen bonding [16], and form a physical hydrogel through the well-known freeze-thaw process [17]. Inherent non-toxicity, non-carcinogenicity, and good biocompatibility represent additional desirable features. Finally, PVOH is the only known purely C—C macromolecule that can be biodegraded [18].

One of the main interests in PVOH-based polymer systems lies in the development of smart devices with tunable release properties. In this respect, long established fields of application are the pharmaceutical and biomedical industries, where PVOH has been extensively used as a privileged polymer for the encapsulation/loading and the subsequent release of enzymes [19], proteins [20], cells [21] and, more broadly, a huge variety of drugs [22–25]. However, the field of sustained delivery of active compounds is advancing rapidly, and new applications within sectors that traditionally lagged behind the aforementioned established fields came about during the last decades.

Among others, novel release systems are expected to grow in the coming years within the food packaging field, due to the increasing interest toward the concept of active packaging [26]. The underlying basic idea is to convey an active molecule (e.g. anitimicrobial, antioxidant, etc.) from the polymeric reservoir to the target body (i.e. the food), maintaining its concentration to a predetermined level over a required time span. This can be

* Corresponding author. Tel.: +39 0250316654; fax: +39 0250316672.
E-mail address: stefano.farris@unimi.it (S. Farris).

0927-7757/$ – see front matter © 2012 Elsevier B.V. All rights reserved.
http://dx.doi.org/10.1016/j.colsurfa.2012.03.054

Paper II

"*Exploiting the nano-sized features of microfibrillated cellulose (MFC) for the development of controlled release packaging*"

Cozzolino C.A., Nilsson F., Iotti M., Piga A., Farris S.

Submitted to the Colloids and Surfaces B: Biointerfaces, 2012

Paper III

'*Wetting enhancer' pullulan coating for anti-fog packaging applications*"

Introzzi L., Fuentes-Alventosa J.M., Cozzolino C.A., Trabattoni S., Tavazzi S., Schiraldi A., Piergiovanni L., Farris S.

Applied Materials & Interfaces, 2012, 4: 3692−3700.

ACS APPLIED MATERIALS & INTERFACES

Research Article

www.acsami.org

"Wetting Enhancer" Pullulan Coating for Antifog Packaging Applications

Laura Introzzi,[†] José María Fuentes-Alventosa,[†,‡] Carlo A. Cozzolino,[†,§] Silvia Trabattoni,[⊥] Silvia Tavazzi,[⊥] Claudia L. Bianchi,[#] Alberto Schiraldi,[†] Luciano Piergiovanni,[†] and Stefano Farris*[,†]

[†]DeFENS, Department of Food, Environmental and Nutritional Sciences, Packaging Division, University of Milan, Via Celoria 2, I – 20133 Milan, Italy

[‡]Centro de Investigación y Formación Agraria "Alameda del Obispo", Instituto de Investigación y Formación Agraria y Pesquera (IFAPA), Avenida Menéndez Pidal s/n. 14004 Córdoba, Spain

[§]STAA, Department of Agriculture, University of Sassari, Viale Italia 39/A, I – 07100 Sassari, Italy

[⊥]Department of Materials Science, University of Milano Bicocca, Via Cozzi 53, I – 20125 Milano, Italy

[#]Department of Chemistry, University of Milan, Via Golgi 19, I – 20133 Milano, Italy

Supporting Information

ABSTRACT: A new antifog coating made of pullulan is described in this work. The antifog properties are discussed in terms of wettability, surface chemistry/morphology, and by quantitative assessment of the optical properties (haze and transparency) before and after fog formation. The work also presents the results of antifog tests simulating the typical storage conditions of fresh foods. In these tests, the antifog efficiency of the pullulan coating was compared with that of two commercial antifog films, whereas an untreated low-density polyethylene (LDPE) film was used as a reference. The obtained results revealed that the pullulan coating behaved as a "wetting enhancer", mainly due to the low water contact angle (~24°), which in turn can be ascribed to the inherent hydrophilic nature of this polysaccharide, as also suggested by the X-ray photoelectron spectroscopy experiments. Unlike the case of untreated LDPE and commercial antifog samples, no discrete water formations (i.e., droplets or stains) were observed on the antifog pullulan coating on refrigeration during testing. Rather, an invisible, continuous and thin layer of water occurred on the biopolymer surface, which was the reason for the unaltered haze and increased transparency, with the layer of water possibly behaving as an antireflection layer. As confirmed by atomic force microscopy analysis, the even deposition of the coating on the plastic substrate compared to the patchy surfacing of the antifog additives in the commercial films is another important factor dictating the best performance of the antifog pullulan coating.

KEYWORDS: *antifog, coating, packaging, pullulan, surface, wetting*

INTRODUCTION

Current food packaging materials are conceived as a multifunctional tool enabling both the shelf life extension and the market penetration of food products. For this reason, besides containment, protection and preservation of foods, there is demand for packaging materials to afford additional properties, some of them not only directly related to food safety but also to a suitable presentation of the product.

One of these properties is the antifog property, which concerns the capability of the packaging material to avoid the forming small droplets of water on the internal side of the packaging film. Fog formation is a consequence of environmental changes in temperature and humidity: a decrease of film surface temperature below the dew point causes the condensation of water vapor present inside the package. The final effect is the appearance of a "foggy" layer that modifies the optical properties of the material, hiding the contents of the package by scattering of the incident light in all directions, due the newly appeared droplets.[1] The nuisance of fogging on plastic films is frequently of concerns in the case of fresh food and minimally processed (washed, trimmed, sliced) vegetables, especially when they are refrigerated after packaging operations. The "see-through" property is actually one of the most important requirements of transparent films, as it can influence the final choice made by consumers. For this reason, it is important to preserve this property, as it can offer a more attractive display of the products throughout the shelf life of the packaged food.

It has been pointed out that the detrimental effect of fog on the transparency of the material mainly depends on the shape of the droplets,[2] which is reflected by the balance between the three

Received: May 4, 2012
Accepted: July 3, 2012
Published: July 3, 2012

Paper V

"*Qualità e sicurezza dei prodotti vegetali minimamente trattati (IV gamma) attraverso imballaggi plastici funzionali*"

Quaderni della Ricerca, 2012, vol. 143. Regione Lombardia Agricoltura.

[VEGAPACK PROJECT]

UNIVERSITÀ DEGLI STUDI DI MILANO
FACOLTÀ DI AGRARIA

CONSIGLIO NAZIONALE DELLE RICERCHE
ISMAC
ISTITUTO PER LO STUDIO DELLE MACROMOLECOLE

UNO LOMBARDIA

Qoasi

www.regione.lombardia.it

QUALITA' E SICUREZZA DEI PRODOTTI VEGETALI MINIMAMENTE TRATTATI (IV GAMMA) ATTRAVERSO IMBALLAGGI PLASTICI FUNZIONALI

VEGAPACK

Quaderni della Ricerca
n. 143 - febbraio 2012

LOMBARDIA. **COSTRUIAMOLA INSIEME**

RegioneLombardia
Agricoltura

AWARDS

University of Burgundy
Institute of Technology of Dijon-Auxerre

7 Blvd Docteur Petitjean - BP17867
210078 DIJON Cedex

Best Poster AWARD

Cozzolino Carlo Alessio

from ***DISTAM University of Milan*** - Italy.

was awarded by the scientific committee of the

2nd International Meeting on
Packaging Material-BioProduct Interaction
(MATBIM 2012 - France, 22-25th April 2012**)**

based on the topic originality, the science and communication qualities

For the organising committee

UNIVERSITE DE BOURGOGNE Département Génie Biologique IUT de DIJON

Prof. F Debeaufort

MATBIM 2012 2nd international meeting on Material/Bioproduct Interaction

Dijon 22-25 April 2012

The first work (Paper I) was presented at the Matbim 2012 conference and it was awarded as the best work in Session 2, Transfers (The mechanisms of permeation, diffusion, migration of gases and common additives in traditional packaging materials (petrol based plastics) are quite well-known, but that of new organic (essential oil, polyol plasticizers…) or inorganic (zeolithes, metal particles, ink components or solvents) added compounds in new materials such as bio-sourced or active material are much less characterized.)